NUCLEAR AEROSOL BEHAVIOUR IN LMFBR

Comparison of Computer Modelling with Aerosol Experiments

J. FERMANDJIAN
DSN/Centre de Fontenay-aux-Roses,
Fontenay-aux-Roses,
France

ABSTRACT

For the purpose of studying the behavior of the concentration of aerosols confined in a vessel, various models have been developed, especially in the United States : HAA 3B, HAARM 2 and HAARM 3 - in the Federal Republic of Germany : PARDISEKO 3 and PARDISEKO 3B - in Japan : ABC 2 and ABC 3 - in the United Kingdom : AEROSIM and in the Netherlands : ETHERDEMO and MADCA.

These codes were validated on the basis of tests conducted in vessels whose volumes varied between 0.022 and 850 m^3. The aerosols studied differed in nature (sodium oxide, fuel oxide, sodium oxide-fuel oxide, gold) and method of production (sodium pool fires, sodium spray fires, arc vaporization , exploding wire) in various atmospheres air, air with variable amounts of oxygen, and nitrogen.

This comparison between calculation and experimental results reveals that difficulties still exist, especially as to the selection of the values to be given to some input parameters of the codes (physical data of experimental origin, in particular, the aerosol source function and the characteristics of the size distribution of the emitted particles). Furthermore, the importance of thermophoresis and convection currents has been proved : including the soaring effect in the ABC 3 code enables to fit the experiment.

INTRODUCTION

Aerosol behavior within Liquid Metal Fast Breeder Reactor (LMFBR) containments is of critical importance since most of the radioactive species are expected to be associated with particulate forms and the mass of radiologically significant material leaked to the ambient atmosphere is directly related to the aerosol concentration airborne within the containment. Mathematical models describing the behavior of aerosols in closed environments, besides providing a direct mean of assessing the importance of specific assumptions regarding accident sequences, will also serve as the basic tool with which to predict the consequences of various postulated accident situations. Consequently, considerable efforts have been recently directed toward the development of accurate and physically realistic theoretical aerosol behavior models.

The primary purposes of this work are to :

. note the general agreement between the predictions and the data,

. identify the codes'adequacy for scaling when geometries or conditions vary,

. assess the conservative nature of the models and assumptions.

I. COMPUTER MODELING OF NUCLEAR AEROSOL BEHAVIOR.

These models have accounted for various mechanisms affecting agglomeration rates of airborne particulate matter as well as particle removal rates from closed systems. In all cases, spatial variations within containments have been neglected and a well-mixed control volume has been assumed. All codes are intended to evaluate the time-dependent airborne radioactivity that aerosols carry inside the reactor building and that may escape to the environment.

Existing computer codes formulated from the mathematical aerosol behavior models are:

ABC 2	[1]	Japan
ABC 3	[2]	Japan
AEROSIM	[3]	U.K
HAARM 2	[4]	USA
HAARM 3	[5]	USA
HAA 3B	[6]	USA
MADCA/ETHERDEMO	[7]	The Netherlands
PARDISEKO 3	[8]	FRG
PARDISEKO 3B	[9]	FRG

II. DESCRIPTION OF THE TESTS

1. Test Vessels

Vessels of the following sizes have been used to study sodium fires.

- CSTF V = 850 m^3
- CEA containment V = 400 m^3
- LTV V = 60 m^3
- NSPP V = 38.3 m^3
- NABRAUS V = 4 m^3
- JAERI containment V = 1 m^3

The following vessels have been used to study fuel aerosol behavior.

- . LTV V = 60 m^3
- . NSPP V = 38.3 m^3
- CRI II V = 4.5 m^3
- TUNA V = 2.2 m^3
- LTC V = 1.13 m^3
- JAERI containment V = 1 m^3
- CRI III V = 0.53 m^3
- Explosion chamber V = 0.022 m^3

Dimensions of the various test vessels are shown in Table I.

2. Aerosol Generation Techniques

Burn pots with surfaces varying from 0.002 to 4.4 m^2 have been used to generate aerosols for sodium pool fires (Table II). Arc vaporization and the exploding wire technique have been used to generate fuel aerosols.

Sodium oxide particles usually had initial count diameters of about 0.1 to 0.5 µm ; fuel aerosols usually had mean diameters of about 0.05 µm. Geometric standard deviations for the particles were generally from 1.5 to 2.5. The particle size determinations have been most often concerned with agglomerates at short times after formation rather than with the initial primary particle size distributions.

3. Measurement Techniques

Table III shows the different measurement techniques used to describe aerosol behavior.

4. Quantities Burned or Released

From 1 g to 470 kg of sodium have been burned in pool fires. Between 0.05 g and 70 kg have been released (Table II). The quantities of fuel oxide vaporized are usually small. The masses released have been between 0.02 g and 160 g.

5. Aerosol Chamber Atmospheres

Sodium pool fires have been conducted with air. In some cases humidities have been controlled and varied. Atmospheres in the containment vessel for fuel aerosol studies are frequently inert (argon or nitrogen).

III. EXPERIMENTAL VALIDATION OF CODE MODELS

Input parameters for the codes are shown in :

- Table IV (sodium oxide aerosols)
- Table V (fuel oxide aerosols)
- Table VI (fuel oxide-sodium oxide aerosols).

1. HAARM-2 sodium oxide aerosols

JAERI tests [10] : Figure 1 compares experimental data from JAERI tests for sodium oxide aerosols. Dashed curves represent experimental results, solid curves predicted values. The experimental curves are for airborne concentrations of three JAERI experiments ; the predictions are based on reported experimental conditions. The agreement is good for the cases shown here, but the predicted values may be too low for long times. Otherwise, the predicted values follow the experimental data but are consistently conservative in that higher concentrations are predicted.

CASSANDRE tests [11] : The application of the HAARM-2 code to the CASSANDRE tests shows a deviation of a factor of 10 or more between the calculation and the experiment (mass concentration as a function of time). Figure 2 shows the relationship to CASSANDRE 03. However, the calculations reproduce the shape of the experimental curves.

The deviation between calculated and measured deposition of aerosols on the floor and on the walls is relatively small (a slight deviation for CASSANDRE 02, 04, and 08 with a greater deviation for CASSANDRE 03, 05 and 07) (Table VII). In the CASSANDRE tests, the particles are deposited on the walls essentially through thermophoresis.

Figures 3 and 4 show the deposited weight of sodium oxide on the floor and on the walls. The settled mass showed good agreement but the diffused mass differed more widely (a factor of about 2 between experiment and calculation).

The HAARM-2 code appears to give reasonably accurate but conservative predictions of aerosol concentrations. Nevertheless, it may underestimate concentrations for long times. The major problems with it are related to inaccurate scaling of vessel size.

Note : Figure 2 also compares HAARM-2 and PARDISEKO 3 calculations. The input assumptions are identical for each code, and the agreement between predictions is excellent. For this case, the assumed log-normal size distribution used in HAARM-2 appears adequate.

2. HAARM-3

• Sodium oxide aerosols

CASSANDRE tests : The application of the HAARM 3 code to the CASSANDRE tests indicates a deviation between the calculation and the experiment (mass concentration vs. time) which is definitely smaller than that obtained with the HAARM 2 calculation (Figures 5 and 6). Figure 6 related to the CASSANDRE 5 test, emphasizes the importance of the accurate knowledge of the median radius and the standard deviation of the distribution of the emitted particles, so that the aerosol source function.

NSPP tests [12] : Figures 7 and 8 show the results of two NSPP experiments (NSPP Run 103 and NSPP Run 104) and comparison of these results with concentrations predicted using the HAARM 3 code. From these figures, it is seen that the agreement between experiment and calculation is excellent for NSPP Run 104, less good (nevertheless conservative) for NSPP Run 103.

CSTF tests [13] : Figure 9 compares the experimental suspended mass concentration in CSTF test AB1 with the HAARM 3 code prediction (brownian diffusional boundary thickness = 10 µm - temperature gradient at the vessel wall = negligible). Good agreement is shown except at the very early times, where the code underpredicts because it does not account for condensation of water vapor. Since the experimental result shows that the maximum aerosol concentration did not reach the expected level, another HAARM 3 calculation way made with a reduced source rate. Figure 9 emphasizes the importance of the aerosol source function. Even when the conditions are well known, as in the present test, there is a large uncertainty in the source rate : need for an accurate method, to forecast the aerosol mass release rate. Figure 10 shows the aerodynamic mass median diameter (suspended particles) vs. time, calculated by HAARM 3 and measured by Andersen cascade impactor and Sierra cascade impactor : important deviation during the fire (up to 60 minutes), then relatively good agreement. It should be noted that the experimental particle size data show a considerable difference between measurements with the two impactor types employed.

• Fuel oxide aerosols (NSPP tests) [12]

Figure 11 compares the HAARM 3 calculations (dynamic shape factor = 3, collision shape factor = 3, density correction factor = 1) with uranium oxide U_3O_8 data for ORNL experiment (NSPP run 201). Since uranium oxide is known to form branched chain-like agglomerates, the dynamic shape factor and the collision form factorwere utilized in the computer calculation.

Furthermore, since no exact information on the source rate was available, two different source rates that match approximately with the measured aerosol concentration at a time of 10 minutes were tried. Taking into account the spread of the experimental results, good agreement between the experiment and the calculation, except that the code underestimates concentrations at long times ($\sim$ 1 day).

3. HAA-3B Sodium oxide aerosols [13]

Figure 12 compares the experimental suspended mass concentration in CSTF test AB1 with the HAA-3B code prediction. Three values for α, the Stokes correction factor, are shown. The code overpredicts the concentration for the critical initial few hours for all three values of α. The base case (α = 0.1, ε = 1.0, r_{50} = 0.5 µm, σ_g = 2.0, ρ = 2.4 g.cm^{-3})gives the best overall fit with the experiment and is conservative. This case predicted 81 % of mass settled, 19 % plated, while the experimental results were 93 % and 7 % (Table VIII). Increasing δ_D (brownian diffusional boundary tickness) from 0.1 to 0.27 gives an accurate prediction of settled and plated mass. The base case also predicted an aerodynamic mass median diameter of 4.4 µm (σ_g = 2.85) at the time of maximum concentration, which is to be compared with 5.5 µm (σ_g = 2.35) by the Andersen cascade impactor. It is concluded that the HAA-3B is capable of giving reasonably accurate predictions with the proper choice of particle properties.

4. PARDISEKO 3

• Fuel Oxide Aerosols in TUNA and Explosion Chamber [15] [16]

The agreement between the TUNA experiments, carried out with UO_2 aerosols in nitrogen, and the PARDISEKO theory was satisfactory if some reasonable assumptions on aerosol form factors are made (see Figure 13). The solid curves are the envelopes of the range ; they represent all experiments carried out in TUNA at room temperature. The best fit was achieved by using f = 8.2 and K = 3.5, which, at least for K, agrees with the comparable literature. The same form factors applied to experiments in TUNA at elevated temperatures also showed good agreement between experiment and theory. For a small chamber (0.022m^3), experiments using the same K and f values gave the best agreement (Figure 14).

The experiments can be divided in three zones of time :

- At the beginning, the brownian agglomeration predominates.
- Later, the agglomeration decreases and settling and diffusion become important.
- Finally, only settling and diffusion act on the particles.

The above mentioned values for f and K are defined such that the theoretical material density should be used in the equations. Since a close relation exists between particle shape factor and particle density the choice of these parameters should be properly defined, in order to avoid the confusion may arise from ambiguous usage in different codes. An agreement between code developers on such definitions would be most valuable.

- Sodium Oxide Aerosols in the CASSANDRE Tests [11]

Applications of the PARDISEKO 3 code to the CASSANDRE tests have been calculated. Figure 2, which compares the time function of sodium oxide aerosol concentration with a PARDISEKO 3 calculation, shows one typical result. Form factors other than the f=1 and K=1 used for UO_2 aerosols should apply. It is not fully understood whether the typical result of PARDISEKO 3 curves being always above the experimental curves is because of the form factors assumed (f=1 and K=1) or because gravitational coagulation was neglected in these calculations.

- Comparison PARDISEKO 3 - HAARM 2 [11]

The assumption of lognormal size distribution (for suspended particles) throughout the considered time period in HAARM 2 poses the problem of proving its validity.

Considering the results obtained (evolution of the mass concentration of the suspended particles) in the case of the CASSANDRE tests, it appears that the performances of PARDISEKO 3 and of HAARM 2 are comparable, which would tend to justify the simplifying assumption used in HAARM 2 in the presence of a long and intense source.

However, significant deviations persist between the two codes, in particular the evolution of the characteristics (median radius and standard deviation) of the size distributions of the suspended particles (Figures 15 and 16).

In the case of the CASSANDRE 2 test (important emission of small and slightly dispersed particles : $r_g = 0.12\ \mu m - \sigma_R \approx 1.5$) the size distribution, calculated by PARDISEKO 3, of the suspended particles, at the end of fire, definitely deviates from the lognormal distribution (Figure 15) with two maxima : the first is due to the existence of the (long and intense) source, the second to the (brownian) agglomeration of the particles.

Furthermore, there exists a significant difference between the calculated results (PARDISEKO 3 and HAARM 2) of the relative distribution of deposited aerosol between walls and floor of the vessel (Table VII and figures 3 and 4), one of the causes of this difference being the use of different deposition equations by the two codes.

5. PARDISEKO 3B Sodium Oxide Aerosols [9]

PARDISEKO 3 has been improved, in particular by leaving out assumptions on size distributions : the aerosol size distribution is regarded as consisting of a number of monodisperse fractions (histogram approach in the new version PARDISEKO 3B).

Since the first comparisons between PARDISEKO 3 calculations with time dependent aerosol sources in larges volumes revealed differences more than a small factor, further calculations for comparison with PARDISEKO 3B have been performed. Figure 17 shows an example of these new comparisons. In the first time region (up to about 50 minutes) the agreement between experiment and calculation (with PARDISEKO 3B) is excellent. In the time region after the calculated mass concentration is still higher (but less high than with PARDISEKO 3). The agreement in the second time region becomes likewise good if the source function is restricted to 60 minutes. This emphasizes the necessity to define more exactly the aerosol source function in any experiment.

A final test whether the theoretical assumption made in a code for aerosol modeling are correct and lead to a description of the real accidental aerosol system with sufficient accuracy can be made only by comparison with experiments. In the frame of the FAUNA program, starting 1978 at Karlsruhe, a larger vessel (230 m^3) will be available to make the necessary experiments to answer that problem.

6. AEROSIM [3]

No systematic comparison has yet been made between AEROSIM and experiments. Figure 18 shows the comparisons with HAA 3B, PARDISEKO 3 and AEROSIM (the same set of input parameters was used in the three codes). It can be seen from the graph that, for the conditions shown (TUNA tests), these programs give similar predictions.

7. ABC-2 [17]

- Sodium Oxide Aerosols (JAERI Tests, Large Test Vessel)

JAERI tests : The concentration decrease between experiments and calculations was compared for four JAERI experiments (Figure 19). Good agreement was obtained for dilute aerosol concentration from 0.01 to 1 g/m^3 in Run 3 and

Run 13. In higher aerosol concentrations, calculated values agreed relatively well with experimental data but resulted in some slight overestimation.

:Table IX shows the final deposited weight of sodium oxide on floor and walls. For the deposition, dilute aerosol concentration tests (Run 3, Run 13) agreed well with the calculations, but high concentration tests (Run 8, Run 10) showed a small difference.

LTV tests:The ABC code was also compared for two LTV experiments. Figures 20 and 21 show that calculations for the change of aerosol concentration over time corresponded relatively well with experimental results except during peak concentration. This discrepancy may be because of the sodium burning rate even though a constant burning rate was used in calculations.

Figure 22 shows the deposited weight of sodium oxide on floor and walls (LTV Test 3). The deviations between experiments and calculations are sometimes important, particularly by a factor of 2 for the platted mass at the end of the test.

- Fuel Oxide Particles and Fuel Oxide-Sodium Oxide Mixed Particles (JAERI Tests).

Figure 23 shows the decrease of concentration of the U_3O_8 aerosol in the test vessel. The attenuation of U_3O_8-Na_2O mixed aerosol concentrations is shown in Figures 24 and 25 where the weight percentages of U_3O_8 were 6.7 % and 85 %, respectively.

For U_3O_8 of 6.7 % weight, experiments and calculations agreed well. For U_3O_8 contents of 85 and 100 % weight, however, the calculations for the change in aerosol concentration over time did not correspond with experimental results. It is assumed that these calculations are based on the liquid drop model, because the calculations agreed well with the behavior of spherical aerosol particles, such as sodium oxide, and the mixed particles of 6.7 % weight of U_3O_8 but do not correspond with the no-sphere particles of 85 and 100 % weight of U_3O_8. (The dynamic shape factor and the fluffiness factor are used to analyse the behavior of chain-like or branched chain-like particles in studies at AI, BCL, and KFK).

It was assumed in the calculations that the Stokes' apparent density of the aggregate was approximately constant after some coagulation was attained. Sodium oxide aerosol particles or sodium oxide mixed with fuel (in small quantities) are rather spherical compared to pure fuel aerosol and have a constant density after a few minutes [18].

8. ABC-3 (in Chimney-Type Chamber with Hot-Plate Heating) [2]

Experiments in Japan obtained information on the thermophoretic deposition and the aerosol soaring in the hypothetical accident. A heated, perpendicular chimney insulated with asbestos stood at the center of the chamber to obtain the ideal thermal convection. The hot-plate heat source was placed on the floor in the same chamber. Therefore, the convection of air occured perpendiculary to the floor, and aerosol settling in the chamber was hampered.

Figures 26 and 27 show that the experiments and the calculations for the ABC-3 code agree satisfactorily using the soaring values. In addition the thermophoretic deposition under the ideal free thermal convection was confirmed by the calculation that combined Brock's equation and the Nusselt-type equation of free thermal convection. Figure 28 shows the average velocity v_T of sodium oxide aerosols resulting from thermophoresis versus the heat flux (W/m^2). Open circles represent the calculations, solid circles the experiment. The relationship between average velocity and heat flux is a nearly straight line.

9. ETHERDEMO [7]

ETHERDEMO calculates aerosol behavior in a locally heated vessel. The model has been validated by a variety of experiments. Among the variables are containment size (0.1 - 20 m^3) and shape, heating geometry, temperature range (R.T. - 700°C), aerosol material (metal oxide, salt nuclei, etc..), and gas (air,nitrogen, helium).

Figure 29 indicates that the calculations and the experiments show good agreement. In all cases when low to moderate initial aerosol mass concentration occurred (0.1 g/m^3 or less), the experimental data showed good agreement, which agrees with the size independence of thermophoresis.

In the hypothetical accidents tested, the horizontal surface would be hot (from decay heat of fission products, combustion heat, etc..). Therefore, thermophoretic forces counteracting gravity would hamper deposition of particles on these surfaces. To investigate the importance of such conditions, decay constants for aerosol removal in a vessel with a heated floor were measured. Figure 30 gives the results. With increased floor temperature the decay constant initially decreases (as aerosol stability increases) because of the effect of gravitational settling. At higher levels of heating power, however, the aerosol deposition is enhanced because thermophoretic deposition becomes overwhelming.

10. MADCA [7]

MADCA describes the mass concentration decay of an aerosol after its introduction in a vessel with a heated layer of liquid on the floor. The model was verified with various containments of different sizes and shapes using condensing atmospheres of sodium vapor and water vapor. Temperatures ranged to 100°C for water and 200°C to 700°C for sodium. Aerosol materials used were metal oxide aggregates (including sodium oxide). In all cases the calculations and the experiments agreed well.

The atmosphere inside an enclosure with a heated laver of liquid on the floor is supersaturated with vapor from the liquid. The supersaturation can be observed simply from the formation of fog after aerosol particles are introduced. This fog formation also explains the increased removal rate of aerosol in condensing atmospheres compared to the rate in dry atmospheres (Figure 31). The particles act as condensation nuclei and may grow to sizes with relatively large gravitational settling rates because of continuous material transport from the evaporating liquid to the particles.

The usefulness of the MADCA model was explored by experiments with aerosols in condensing vapors of either water or sodium (in a vessel filled with air or nitrogen). Experiments using aerosols mainly from exploding wire showed that $C_m^{2/5}$ decays linearly with time (Figures 32 and 33)in the SAUNA rig, which is specially built for aerosol experiments in condensing sodium vapor. Sodium oxide aerosol formed in SAUNA decayed as the result of flushing in nitrogen, in this case without the aerosol formed by exploding wire. These data also show a linear decay of $C_m^{2/5}$ (Figure 34).

IV. CONCLUSIONS

The ETHERDEMO and MADCA models are very simple and therefore useful tools for calculations of aerosol safety.

The HAA 3B code is capable of giving reasonable accurate predicting with adequate values for input parameters (form factor , brownian diffusional boundary thickness).

PARDISEKO 3 and HAARM-2 can satisfactorily describe the time function of an instantaneously formed aerosol concentration in a small vessel if some reasonable assumptions (form factors, etc..) are made. HAARM-2 tend to underestimate concentrations at long times ; however, at these times concentrations are very low and have little impact on mass leakage considerations.

The first comparisons between PARDISEKO 3 and HAARM-2 calculations with time-dependent aerosol sources in large volumes showed larger differences.

Reasonable agreement between experiments and calculations (PARDISEKO 3B and HAARM-3) if the source function is reduced. This emphasizes the necessity to definite more exactyl the aerosol source function in any experiment.

Experiments and ABC-2 calculations showed good agreement in a dilute concentration such as 0.1 g/m^3 of sodium oxide aerosol. However, calculations in higher concentration showed small discrepancies.

For the behavior of aerosols of mixed particles of fuel oxide-sodium oxide, ABC has been compared with the low weight of fuel materials like the 6.7 percent U_3O_8-93.3 percent Na_2O system. For fuel oxide aerosols, the change in time lapse of aerosol concentration in calculations does not correspond with experimental results. It is assumed therefore that the ABC code based on the liquid drop model is not adequate for fuel oxide aerosols (chain-like particles).

The ABC-3 code, which includes the soaring effect, shows the importance of thermophoresis and convection currents to explain the experiment.

V. RECOMMENDATIONS FOR RELATED RESEARCH

- Since the aerosol system in a core disruptive accident is formed of several sources (UO_2, PuO_2, Na, fission products, Na_2O, structural elements, etc..),the interaction of these sources must be taken into account. More experimental information on the chemical and physical characteristics of these sources (mean radius and geometric standard deviation of the distribution of the emitted particles, rate of emission of the particles) and the developing aerosol system (mixed aerosol) are necessary.

- It is known that in large vessels (reactor containments), thermal convection (resulting from the decay heat of fission products, combustion heat, etc..) and condensation of sodium vapor (or water vapor) play a significant role. The influence of these effects needs to be investigated and incorporated in present aerosol modeling theories. In particular, the code should include a provision for multiple containment zones resulting from the unhomogeneous distribution of aerosols in the containment in temperatures of gas phases and structures, according to the accidents.

- Experimental confirmation of models for behavior of aerosol from several overlapping sources is not yet sufficient. Data should be provided for large containment volumes (with sources of different nature and duration during the same test).

- Experiments must be as realistic as possible. In particular, simulating high aerosol mass concentrations assumed to be formed by an HCDA requires additional stirring to keep the aerosol spatially homogeneous in the container. Since long-term behavior of the aerosol in such a situation will be influenced by thermophoretic deposition, the computer code must contain the proper equation for thermophoretic deposition.

- Experimental studies of high mass concentration aerosols in containments are necessary in view of :
  - improved insight in relative importance of various typical processes,
  - the possibility of unhomogeneous spatial filling of the containment, under these conditions.

- Thermophoresis results in aerosol removal on cold walls, but it also hampers aerosol deposition onto warm containment walls. Presence of heat-producing debris on horizontal surfaces of containments will hamper deposition of particles on these surfaces because of the ther-

mophoretic forces counteracting the deposition. As long as this increased aerosol stability as it may arise under postaccident conditions in a reactor containment has not been thoroughly studied, application in a code of stirred gravitational settling may be non conservative. In addition, the basic equation of aerosol behavior should include the soaring effect to accommodate instances such as the soaring effect of a sodium pool over the entire surface of the floor of the vessel.

- Trace-level fission product behavior and radiation effects should be studied.
- Need for all codes to be compared against the same experiment (in particular, comparison of particle size distribution).

ACKNOWLEDGMENTS

This work was carried out in the frame of the experts group on nuclear aerosol in reactor safety (under the chairmanship of M. Mel SILBERBERG of USNRC) established by the CSNI at the 1977 annual meeting. One of the first tasks of the group was to prepare a state-of-the-art report on nuclear aerosols in reactor safety.

The author wish to thank for their contribution :

. M. Mel SILBERBERG (NRC - USA)

. M. Frank ABBEY (UKAEA - UK)

. M. Kikuo AKAGANE (PNC - JAPAN)

. Dr. James A. GIESEKE (BCL - USA)

. Dr. Robert K. HILLIARD (HEDL - USA)

. M. Susumu KITANI (JAERI - JAPAN)

. Dr. Tom S. KRESS (ORNL - USA)

. Dr. W.O. SCHIKARSKI (GfK - FRG)

. Dr. Werner SCHOCK (GfK - FRG)

. Dr. Joop VAN de VATE (ECN - The Netherlands)

REFERENCES

[1] G. NISHIO et al.
Evaluation of plutonium oxide aerosol release from an LMFBR in a hypothetical accident.
Vol.34, n°3, 1975 pp.417-428.

[2] G. NISHIO et al.
Sodium oxide aerosol behavior in a closed chamber under thermal convection flow.
Private communication March 1978.

[3] B.C. WALKER et al.
Discretization and integration of the equation governing aerosol behavior.
SRD R 98 July 1978.

[4] L.D. REED et al.
HAARM-2 users manual.
BMI-X-665 October 1975.

[5] J.A. GIESEKE et al.
HAARM-3 users manual.
BMI-NUREG-1991 January 1978.

[6] R.S. HUBNER et al.
HAA-3 user report.
AI AEC 13088 March 1973.

[7] J.F. VAN de VATE
Deposition of aerosols formed by HCDA due to decay heat transport in LMFBR inner containment atmospheres.
International meeting on fast reactor safety and related physics.
October 5-8, 1976, Chicago.

[8] H. JORDAN et al.
PARDISEKO 3. A computer code for determining the behavior of contained nuclear aerosols.
KFK 2151 May 1975.

[9] H. BUNZ
PARDISEKO 3B code.
Private communication 1978.

[10] J.A. GIESEKE et al.
Aerosol behavior modeling and measurements.
IWGFR (IAEA)
Specialist's meeting on "Aerosol formation, Vapour deposits and Sodium vapour trapping".
December 13-17, 1976, Cadarache. pp. 134-142.

[11] J. FERMANDJIAN
Interprétation des essais CASSANDRE au moyen des codes de calcul PARDISEKO 3 et HAARM 2.
Private communication 1977.

[12] J.A. GIESEKE et al.
Aerosol measurements and modeling for fast reactor safety.
Quarterly progress report for october-december 1977.
NUREG/CR-0084 BMI-1999 May 1978.

[13] J.A. GIESEKE et al.
Aerosol measurements and modeling for fast reactor safety.
Annual report for FY 1977
BMI-NUREG.1989 December 1977.

[14] R.K. HILLIARD
Sodium oxide/hydroxide aerosol properties and behavior in a large vessel..
15th DOE Nuclear Air Cleaning Conference.
August 7-10, 1978, Boston.

[15] W.O. SCHIKARSKI
On the state of the art in aerosol modeling for LMFBR safety analysis.
International meeting on fast reactor safety and related physics.
October 5-8, 1976, Chicago.

[16] H. JORDAN et al.
Nukleare Aerosole in geschlossenen System.
KFK 1989 August 1974.

[17] K. AKAGANE et al.
Analysis of aerosol behavior for fast reactor safety.
Private communication March 1978.

[18] G. NISHIO et al.
Measurement of aerosol density of sodium oxide, uranium oxide and their mixed aerosols.
Private communication March 1978.

GLOSSARY OF ACRONYMS USED

ABC	Aerosol Behavior in Containments
AEROSIM	Aerosol Simulator
AI	Atomics International
BCL	Battelle Columbus Laboratories
CEA	Commissariat à l'Energie Atomique
CRI	Containment Research Installation
CSTF	Containment Systems Test Facility
ECN	Energieonderzoek Centrum Nederland
ETHERDEMO	ECN Thermophoretic Deposition Model
FAUNA	Forschungs anlage zur Untersuchung
FRG	Federal Republic of Germany
HAARM	Heterogeneous Aerosol Agglomeration Revised Model
HEDL	Hanford Engineering Development Laboratory
JAERI	Japan Atomic Energy Research Institute
KFK	Kernforschungszentrum Karlsruhe
LMFBR	Liquid Metal Fast Breeder Reactor
LTC	Laboratory Test Chamber
LTV	Large Test Vessel
MADCA	Model for Aerosol Decay in Condensing Atmospheres
NABRAUS	Natrium brand und Schwebstoffilter anlage
NSPP	Nuclear Safety Pilot Plant
ORNL	Oak Ridge National Laboratory
PARDIKESO	Partikeln Diffusion Sedimentation Koagulation
TUNA	Teststand zur Untersuchung nuclearer Aerosole
USA	United States of America

Country	Institute	Vessel chamber	Volume(m^3) V	Height(m) H	Diameter(m) Ø	Floor Area(m^2) A_F (a)	Wall area(m^2) A_W (b)	$A'_F/V(m^{-1})$ (c)	$A'_W/V(m^{-1})$ (d)
USA	HEDL	CSTF	850	20.3	7.62	88	1000	0.10	1.18
	AI	LTV	60	9	3.05	6.6	77	0.11	1.28
	ORNL	NSPP	38.3	5.49	3.05	7.7	68.9	0.20	1.80
	ORNL	CRI II	4.5	2.04	1.68	2.2	11.7	0.49	2.6
	AI	LTC	1.13	1.8	0.9	0.63	10.3	0.56	9.1
	ORNL	CRI III	0.53	0.63	1.03	0.84	3.2	1.57	5.9
	HACL	Test cell	90						
FRG	KFK	FAUNA	200	7	6	28	188	0.14	0.94
		NABRAUS	4	5	1	0.8	17.3	0.2	4.33
		TUNA	2.22	2.9	1	0.78	8.8	0.35	3.96
		Explosion chamber	0.022	0.34	0.3	0.065	0.5	2.94	22.7
JAPAN	JAERI	-	1	2	0.8	0.5	6.27	0.5	6.27
		Chimney-type chamber	1	2	0.8	1.5	6.27	1.5	6.27
FRANCE	CEA	-	400	7.6	-(box)	54	336	0.135	0.84
The Netherlands	ECN	ENAK	20	4.2	2.46	4.76	42	0.24	2.1
		100	1.2	1.5	1	0.8	6.3	0.67	5.3
		200	1	1	-(box)	1	5.5	1	5.5
		GRACE	0.3	1.2	0.56	0.25	2.6	0.83	8.7
		PERVEX	0.15	0.6	-(box)	0.25	1.6	1.67	10.7
		SAUNA	0.15	0.6	0.56	0.25	1.6	1.67	10.7
		300	0.075	0.5	-(box)	0.15	1	2	13.3

(a) Floor area (c) based on total horizontal surface

(b) Wall area (d) Based on total internal surface

TABLE I - CONTAINMENT DIMENSIONS

NOMENCLATURE

A_F : floor aera of the containment

A_W : wall area of the containment

K : dynamic shape factor

T : containment gas temperature

V : containment volume

f,Y : collision shape factor

k_s : thermal conductivity of the particle

p : containment gas pressure

r_g : median radius of the number distribution (particle source)

r_{so} : median radius of the mass distribution (particle source)

α : Stokes correction factor

δ_D, Δ : thickness of boundary layer for brownian diffusion

δ_T : thickness of boundary layer for thermophoresis

ε : collision efficiency of gravitational agglomeration

η : viscosity of air

ρ : density of particle

σ_R : standard deviation of the number/mass distribution (particle source) based on radius

∇_T : temperature gradient in the gas at the containment wall

Vessel name	Test	Sodium mass kg	Combustion area m^2	Fire duration s	Max. aerosol concentration g/m^3	Aerosol formation rate $kgNa/m^2.h$
CSTF V = 850 m^3	AB1	410	4.4	3600	79	as Na_2O_2
	AB2	472	4.4	3600	77	
	AB3*	46	x	140	92	
CEA V = 400 m^3	C2	14	1	2400	11	as Na_2O_2
	C3	42	1	4800	39	
	C4	82	1	7800	83	
	C5	115	1	10800	117	
	C7	300	2	15600	303	
	C8	301	4	7200	244	
LTV V = 60 m^3	2	11	0.56		52	as Na_2O
	3	20	0.56	3800	180	
	5	22.5	0.56	4200	86.5	
	6	22.5	0.56	1200	0.72	
NABRAUS V = 4 m^3	A1(21%O_2)	2	$0.76.10^{-3}$	360	15	as Na
	A2(21%O_2)	2	$4,8.10^{-3}$	840	30	
	A3(43%O_2)	2	$2,1.10^{-3}$	480	8	
	A4(10%O_2)	2	$0,9.10^{-3}$	360	6	
	A5(0,8%O_2)	2	$3,1.10^{-3}$	3600	7	
JAERI V = 1 m^3	3	$9.8.10^{-3}$	0.002	60	0.62	as Na_2O
	8	$18.6.10^{-3}$	0.002	380	6.5	
	10	$40.6.10^{-3}$	0.002	420	9.7	
	13	$0.41.10^{-3}$	0.002	60	0.04	
	Chimney	$0.5.10^{-3}$-$1.5.10^{-3}$			0.07	
	hot-plate	$0.5.10^{-3}$-$1.5.10^{-3}$			0.07	
NSPP V = 38,3 m^3	101	1.1	0.81	240	7.3	as Na_2O_2
	102	5.1	0,81	780	30.5	
	103	5.0	0.81	780	37.3	
	104	10.1	0.81	1260	49.1	
	105*	5.0	x	240	170.0	

* Spray fire

TABLE II - SODIUM FIRES (characteristics)

Aerosol nature	Institute	Vessel name	Number concentration	Mass concentration	Particle size distribution
Sodium oxide	AI	LTV, LTC		filter (gravimetry), filter (radioactive tracer)	Cascade impactor (Andersen-Lovelace), electrostatic precipitator, Royco particle size analyser
	ORNL	NSPP	CNC*	filter [(1)-(2)]	Cascade impactor
	HEDL	CSTF		filter [(1)-(2)-(3)]	Cascade impactor
	JAERI			light scattering device, filter (atomic absorption spectrometry)	thermal precipitator (Zeiss Particle Size Analyser)
	CEA				thermal precipitator (Classimat)
Fuel oxide	AI	LTV, LTC			cascade impactor
	ORNL	CRI-II	CNC	filter (gravimetry)	cascade impactor (Andersen-Low Pressure)
		CRI-III	CNC	filter (gravimetry)	Whitby aerosol analyser (electrical mobility)
	KFK	TUNA	CNC	filter (gravimetry, fluorimetry, activity)	laser aerosol spectrometer, electrostatic precipitator Point-to-Plane (Zeiss Particle Size Analyser)
		Explosion chamber	CNC		
	JAERI		-	filter (photoelectric calorimetry)	
Gold	ECN	200	CNC (Gardner)	filter (radioactive tracer)	Stöber spiral centrifuge
	ENAK		electrostatic precipitator + electron microscope		electrostatic precipitator Morrow and Mercer (Zeiss Particle Size Analyser)

TABLE III - Instrumental analytical techniques for describing aerosol behaviour.

* CNC : condensation nuclei counter.

(1) gravimetry (2) atomic absorption spectrometry (3) alkalimetry

Vessel name or (institute)	Test number	Code	A'_F/V (m^{-1}) (a)	A'_W/V (m^{-1}) (b)	α or(K)	ε	δ_D (μm)	δ_T (μm) or $\lvert\nabla T\rvert$ (°K/cm)	ρ (g/cm^3)	rg (μm)	σ_R	Aerosol released time(s)	Released concentration (g/m^3)
CSTF V=850m^3	AB1	HAA 3B	0.10	1.18	0.1	1	0.1	(0)	2.4	0.12	2.0	3600	79
		HAARM 2	-	-	f(t)	f(t)			-	-	-	-	-
		HAARM 3	-	-	-	-	10	(0)	-	-	-	-	-
	AB2	HAA 3B	-	-			0.1	(0)	1.53	-	-	3600	as Na_2O_2 77
		HAARM 2	-	-	f(t)	f(t)						-	-
		HAARM 3	-	-	-	-						-	-
	AB3 (c)	HAA 3B	-	-			0.1		2.4	0.12	2.0	140	92
(CEA) V=400m^3	C2		0.135	0.84	1	0	100	1000	2.8	0.12	1.5	2400	11
	C3		-	-	-	-	-	-	-	0.51	2.16	4800	39
	C4	HAARM 2	-	-	-	-	-	-	-	0.18	2.11	7800	83
	C5	PARDISEKO 3	-	-	-	-	-	-	-	0.36	2.28	10800	as Na_2O_2 117
	C7	HAARM 3	-	-	-	-	-	-	-	0.22	1.86	15600	303
	C8	PARDISEKO 3B	-	-	-	-	-	-	-	0.14	2.50	7200	244
LTV V=60 m^3	2	HAARM 1	0.11	1.28	f(t)	f(t)	100	(0)	2.27	0.12	2	1000	52
		ABC2	-	-			-	f(t)				-	-
	3	HAARM 1	-	-	f(t)	f(t)	-	(0)	2.27	0.12	2	3780	180
		ABC2	-	-			-	f(t)				-	as Na_2O -
	5	HAARM 1	-	-	f(t)	f(t)	-	(0)	2.27	0.12	2	1200	86.5
	6	HAARM 1	-	-	f(t)	f(t)	-	(0)	2.27	0.12	2	1800	0.72
(JAERI) V= 1 m^3	3	ABC2	0.5	6.27			100	f(t)	0.3	0.5	1.7	60	0.62
		HAARM 1	-	-	f(t)	f(t)	-	(0)	2.27	0.12	2	-	-
		HAARM 2	-	-	f(t)	f(t)	-	(0)	2.27	0.12	2	-	-
	8	ABC2	-	-			-	f(t)	0.3	0.5	1.7	380	6.5
	10	ABC2	-	-			-	f(t)	0.3	0.5	1.7	420	9.7
		HAARM 1	-	-	f(t)	f(t)	-	(0)	2.27	0.12	2	-	-
		HAARM 2	-	-	f(t)	f(t)	-	(0)	2.27	0.12	2	-	as Na_2O -
	13	ABC2	-	-			-	f(t)	0.3	0.5	1.7	60	0.04
		HAARM 1	-	-	f(t)	f(t)	-	(0)	2 27	0.12	2	-	-
		HAARM 2	-	-	f(t)	f(t)	-	(0)	2.27	0.12	2	-	-
	chimney	ABC3	1.5	6.27			-	f(t)	0 6	0,16	1.9		0.070
	hot-plate	ABC3	-	-			-	f(t)	0.6	0,16	1.9		0.07
NSPP V = 38.3 m^3	101		0.2	1.8	f(t)	f(t)		f(t)		0.12	2	240	7.3
	102		-	-	-	-		f(t)		0.12	2	780	30.5
	103	HAARM 3	-	-	-	-		f(t)		0.12	2	780	as Na_2O_2 37.3
	104 (c)		-	-	-	-		f(t)		0.12	2	1260	49.1
	105		-	-	-	-		f(t)				240	170.1

(a) Based on total horizontal surface (b) Based on total internal surface (c) spray fire

TABLE IV- INPUT PARAMETERS (sodium oxide aerosols)

Vessel name or institute	Test number	Code	A'_F/V (m^{-1})	A'_W/V (m^{-1})	α or(K)	ε	δ_D (μm)	δ_T (μm) or $\lvert\nabla T\rvert$ (°K/cm)	ρ (g/cm^3)	rg (μm)	σ_R	Aerosol released time(s)	Released concentration (g/m^3)	Vessel atmosphere	Aerosol formation process	Aerosol nature
LTV V= 60m^3	UAM-72-1	HAARM 1	0.11	1.28	f(t)	f(t)	100	(0)	11	0.05	2	60	2.8	10%[O_2]	arc vaporization	UO_2
NSPP V = 38.3 m^3	201	HAARM 3	0.2	1.8	(3.0)				7.3	0.015	1.5	300			burning metal rod	U_3O_8
	202	HAARM 3														
CRI-II V= 4.5m^3		HAARM 2	0.49	2.6												
TUNA V= 2.22m^3		PARDISEKO 3	0.35	3.96	(3,5)	0	100	3200	11	0.02	1.5	1	0,01	nitrogen	exploding wire technique	UO_2
		HAARM 2	-													
LTC V= 1.13m^3	1U	HAARM 1	0 56	9.1	f(t)	f(t)	100	(0)	7.3	0.05	2	45	0.27		arc vaporization	U_3O_8
	2U	HAARM 1	-	-	-	-	-	-	-	-	2	45	2.4	air		
	7I-1	HAARM 1	-	-	-	-	-	-	-	-	2	75	40.7			
JAERI V= 1 m^3	100 % U_3O_8	ABC 2	0 5	6.27			100	f(t)	0.6	0.3	1.9	30	0.2	air	arc melting	U_3O_8
CRI-III V= 0.53m^3		HAARM 2	1.57	5.9												
Explosion chamber V= 0.022m^3		PARDISEKO 3	2.94	22.7	(3.5)	0	100	3200	11	0.02	1.5	1	1	nitrogen	exploding wire technique	UO_2
		HAARM 1	-		f(t)	f(t)	-	(0)	11	0.05	2	1	1.8			

TABLE V - INPUT PARAMETERS (fuel oxide aerosols).

Vessel name or (institute)	Test number	Code	$A_{F/V}$ (m^{-1})	$A_{W/V}$ (m^{-1})	α	ε	δ_D (μm)	δ_T (μm)	ρ (g/cm^3)	rg (μm)	σ_R	Aerosol released time(s)	Released concentration (g/cm^3)
(JAERI) V = 1 m^3	6.7 % U_3O_8 93.3 % Na_2O	ABC2	0.5	6.27		0	100	f(t)	0.3	0.65	1.8		0.5
	85 % U_3O_8 15 % Na_2O	ABC2	0.5	6.27		0	100	f(t)	2.7	0.25	1.7		0.5

TABLE VI - INPUT PARAMETERS (fuel oxide - sodium oxide aerosols)

Test	Settled mass / Total mass aerosols (%)			Diffused mass / Total mass aerosols (%)		
	EXPERIMENT	PARDISEKO 3	HAARM 2	EXPERIMENT	PARDISEKO 3	HAARM 2
CASSANDRE 02	84	86	77	16	14	23
CASSANCRE 03	79	92	89	21	8	11
CASSANDRE 04	78	76	71	22	24	29
CASSANDRE 05	77	86	84	23	14	16
CASSANDRE 07	74	66	52	26	34	48
CASSANDRE 08	65	68	59	35	32	41

TABLE VII- COMPARISON BETWEEN EXPERIMENT (CASSANDRE) AND CALCULATION (PARDISEKO 3 and HAARM 2) (settled mass and diffused mass).

Test	Settled mass / Total mass aerosol (%)		Diffused mass / Total mass aerosol (%)	
	EXPERIMENT	HAA 3B	EXPERIMENT	HAA 3B
CSTF test AB1	92	85	8	15
CSTF test AB2	93	85	7	15

TABLE VIII-COMPARISON BETWEEN EXPERIMENT (CSTF) AND CALCULATION (HAA 3B) (settled mass and diffused mass)

Test	Settled mass / Total mass aerosol (%)		Diffused mass / Total mass aerosol (%)	
	EXPERIMENT	ABC 2	EXPERIMENT	ABC 2
JAERI Run 3	58	72	42	28
JAERI Run 8	84	66	16	34
JAERI Run 10	51	73	49	27
JAERI Run 13	68	70	32	30

TABLE IX - COMPARISON BETWEEN EXPERIMENT (JAERI) AND CALCULATION (ABC 2) (settled mass and diffused mass)

COMPARISON OF HAARM 2 AND EXPERIMENTAL RESULTS FOR SODIUM OXIDE AEROSOLS IN SMALL VESSEL (JAERI TESTS)

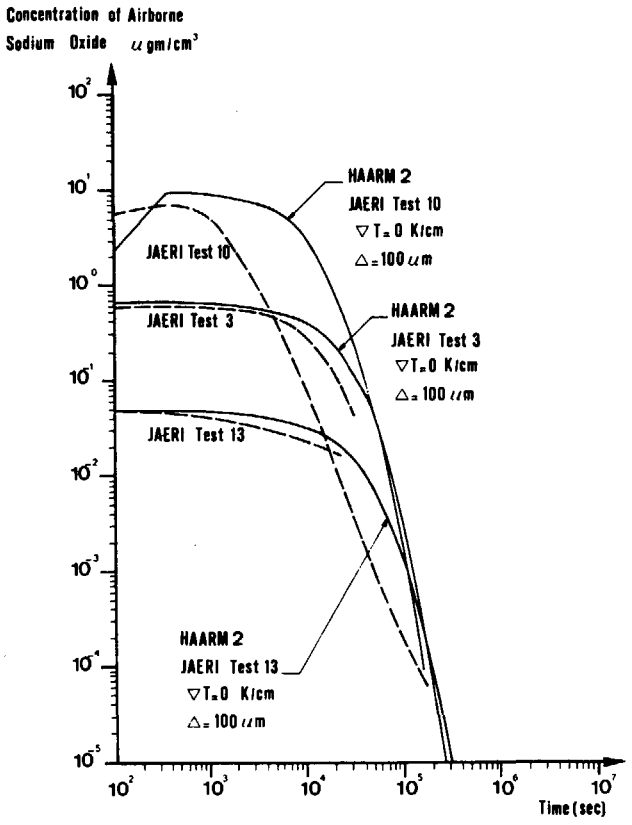

COMPARISON PARDISEKO 3-HAARM 2

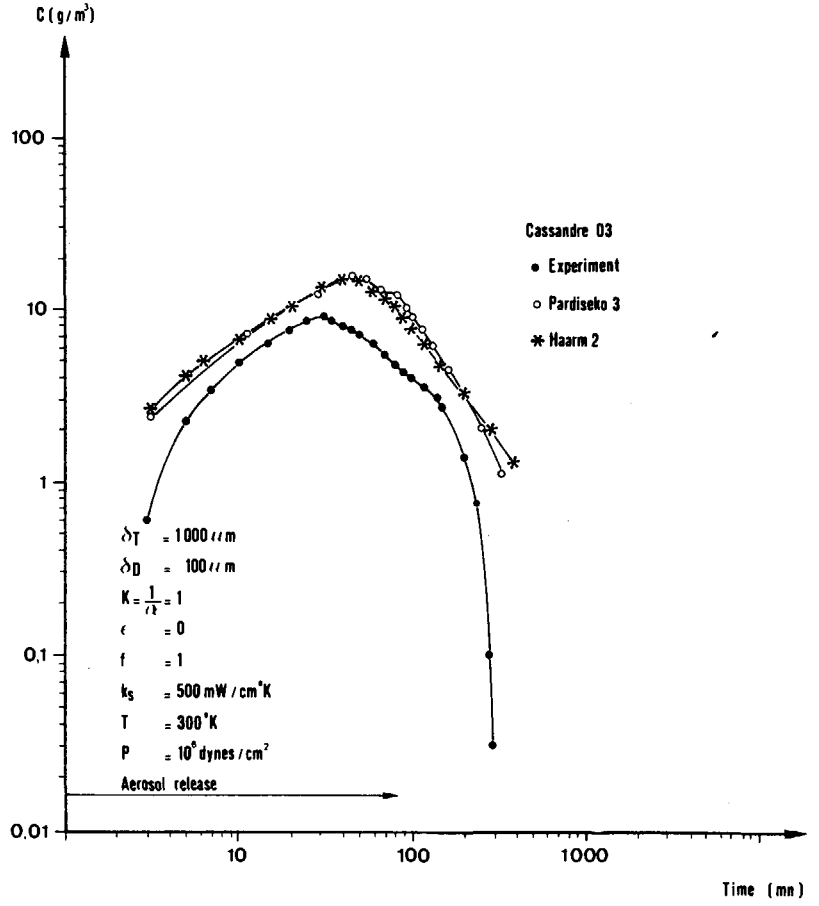

SETTLED MASS VS. TIME

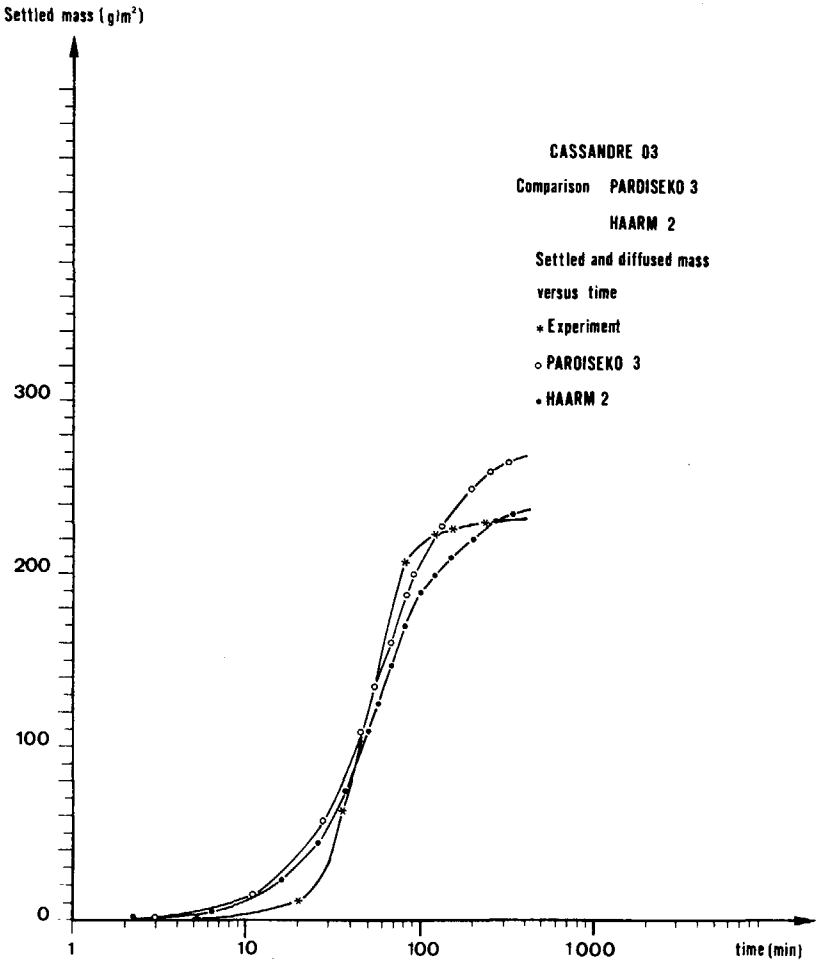

DIFFUSED MASS VS. TIME

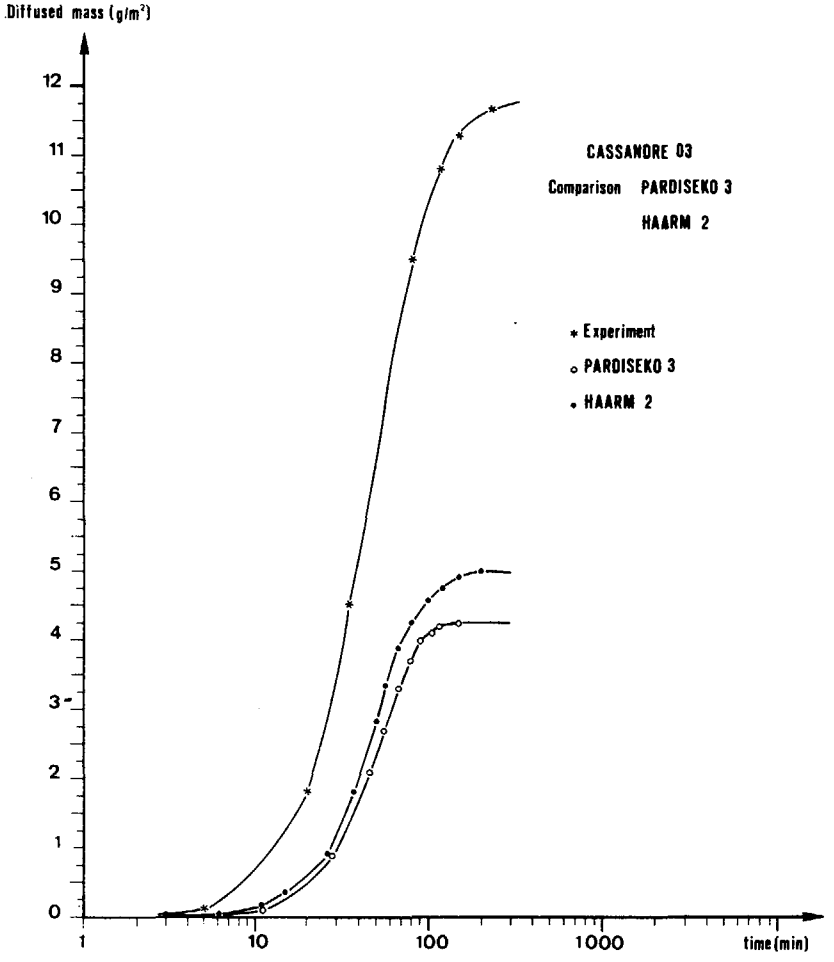

Fig:5

PREDICTED AND MEASURED AEROSOL CONCENTRATION FOR CASSANDRE 4 TEST

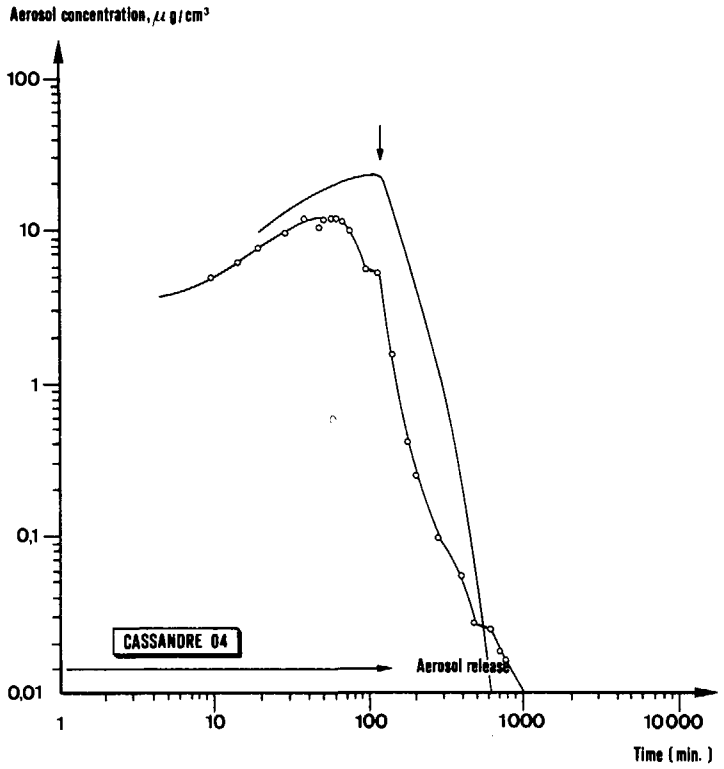

Sodium aerosol: 19.5 kg
Source duration: 130 min
R_{50} = 0.985 μm
σ_R = 2.11

HAARM 3

◇———◇ Experiment

Fig:6

PREDICTED AND MEASURED AEROSOL CONCENTRATION FOR CASSANDRE 5 TEST

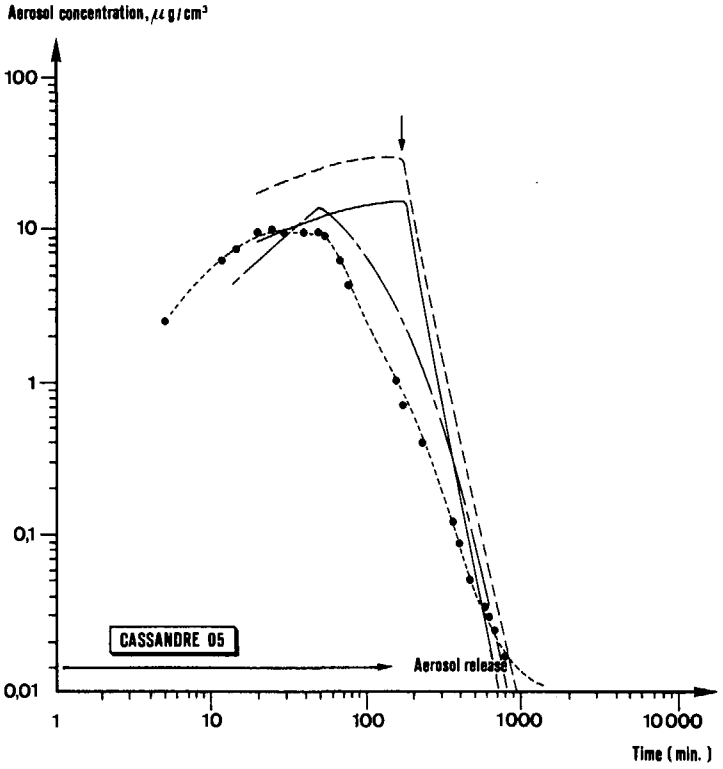

Sodium aerosol: 27.7 kg
Source duration: 180 min
R_{50} = 2.762 μm
σ = 2.28

HAARM-3
HAARM-3 (R_{50} = 0.5, σ_R = 2)
HAARM-3 (R_{50} = 0.5, σ_R = 2)
(Reduced source)

●———● Experiment

Fig:7

COMPARISON OF THE HAARM 3 CALCULATION RESULT WITH EXPERIMENTAL DATA FOR NSPP RUN 103

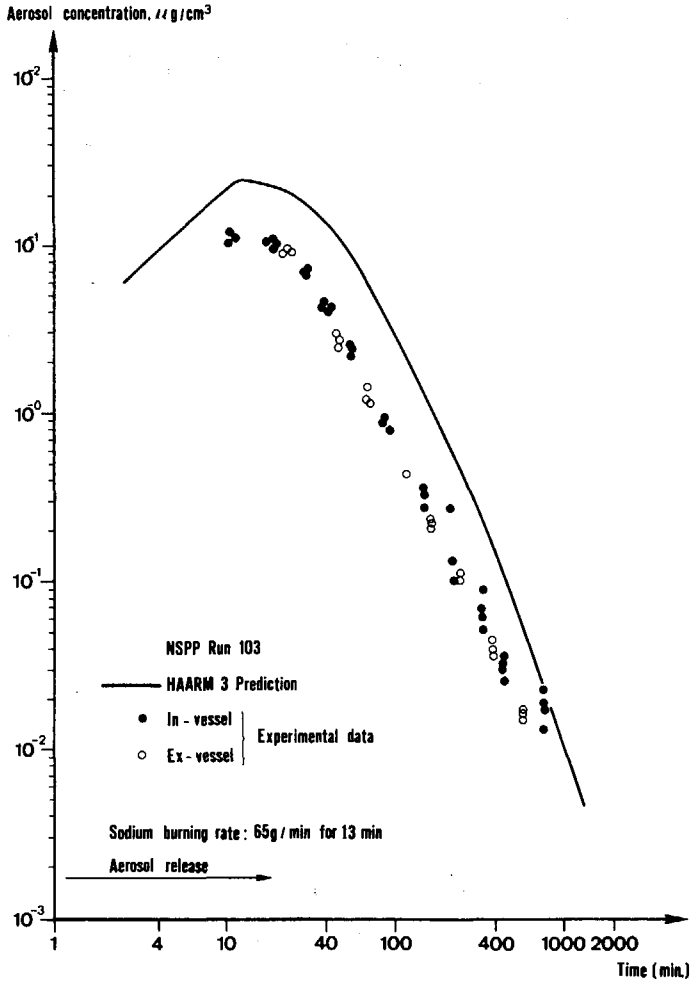

Fig:8

COMPARISON OF THE HAARM 3 CALCULATION RESULT WITH EXPERIMENTAL DATA FOR NSPP RUN 104

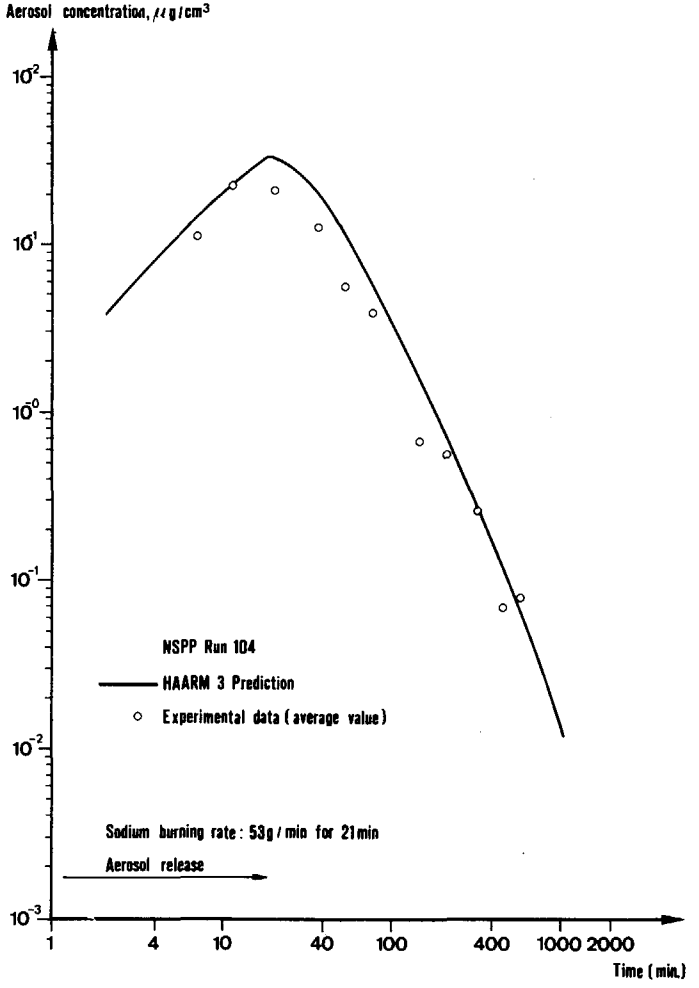

Fig: 9

PREDICTED AND MEASURED AEROSOL CONCENTRATION FOR CSTF RUN AB-1

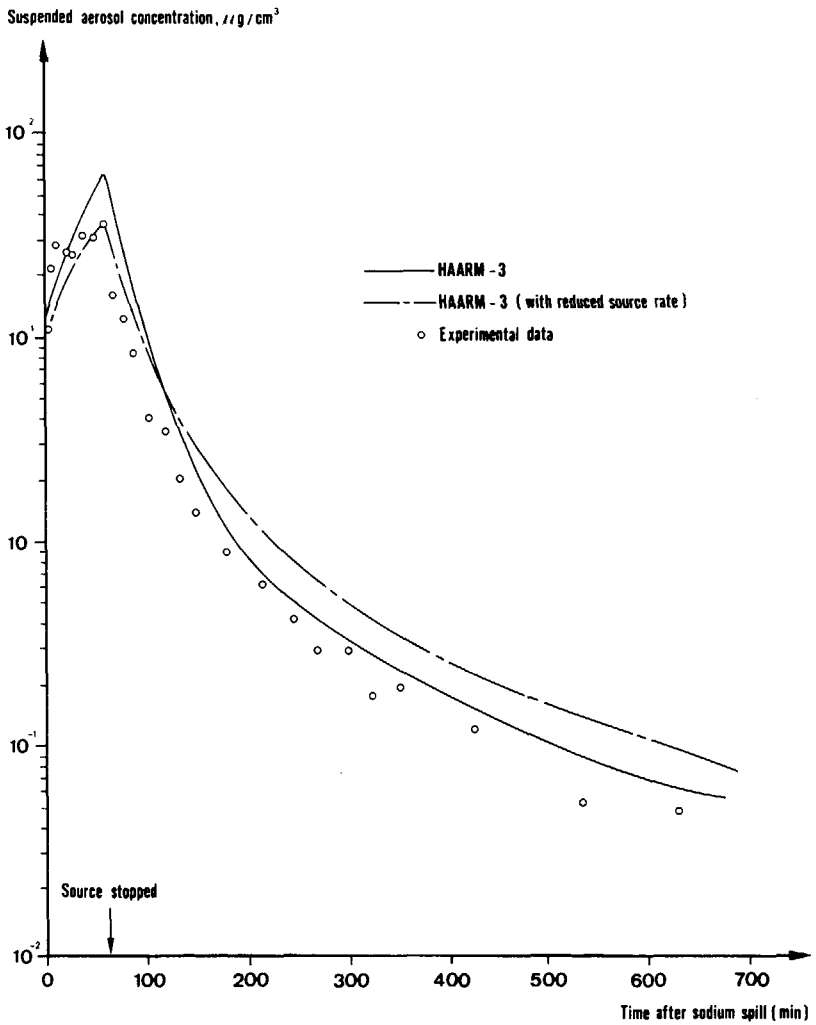

Fig: 10

COMPARISON OF PREDICTIONS AND EXPERIMENTAL RESULTS OF PARTICLE SIZE FOR CSTF AERODYNAMIC MASS MEDIAN DIAMETER VS. TIME

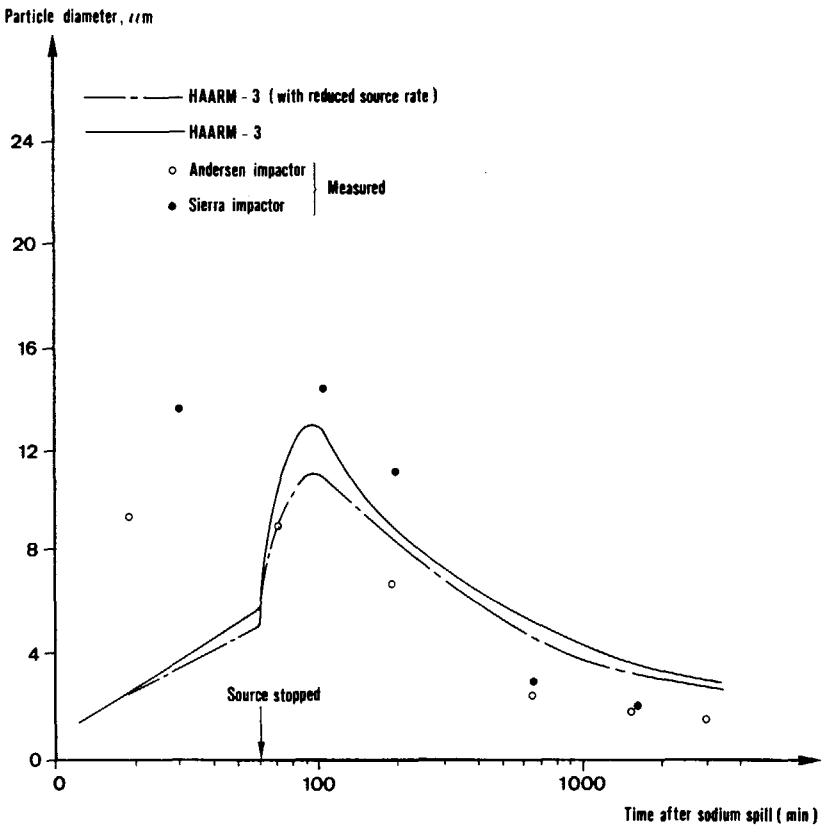

Fig:11

COMPARISON OF THE HAARM-3 CALCULATIONS WITH URANIUM OXIDE AEROSOL DATA FOR ORNL EXPERIMENT NO. 201 (NSPP)

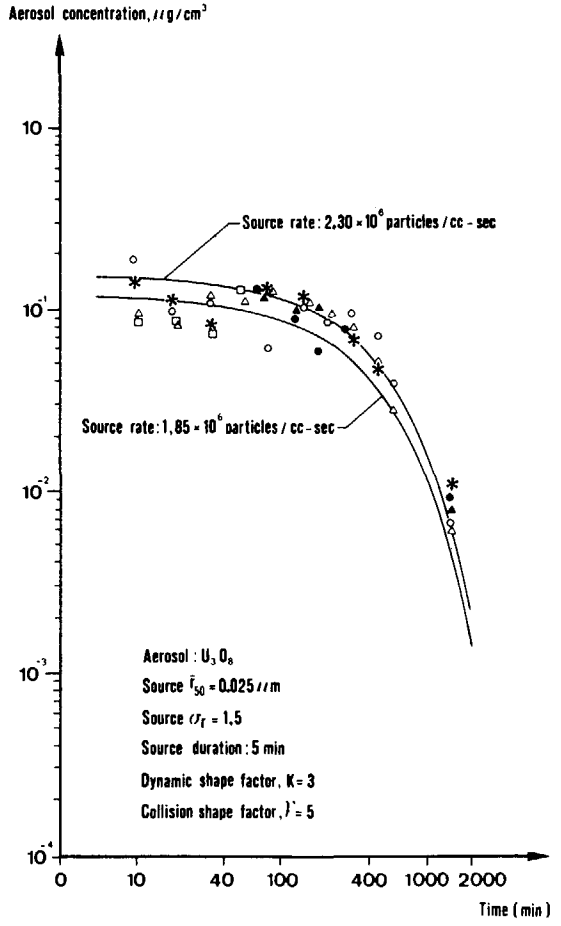

Fig.12

COMPARISON OF HAA_3B COMPUTER CODE PREDICTIONS WITH EXPERIMENT (AB1 test)

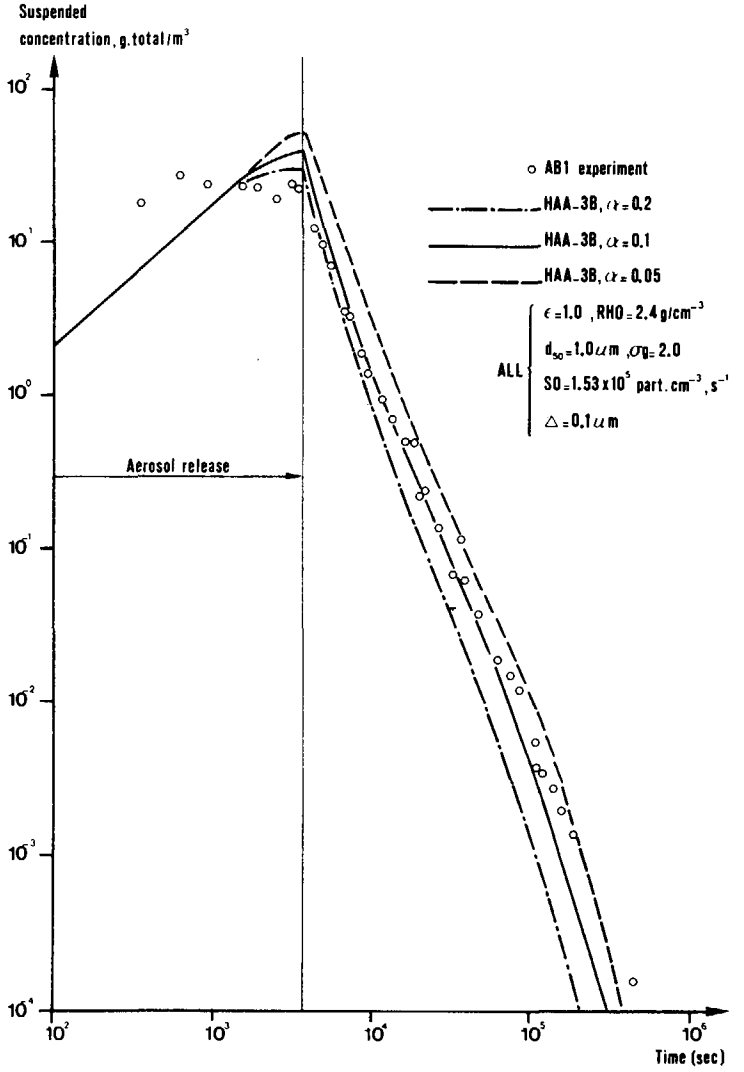

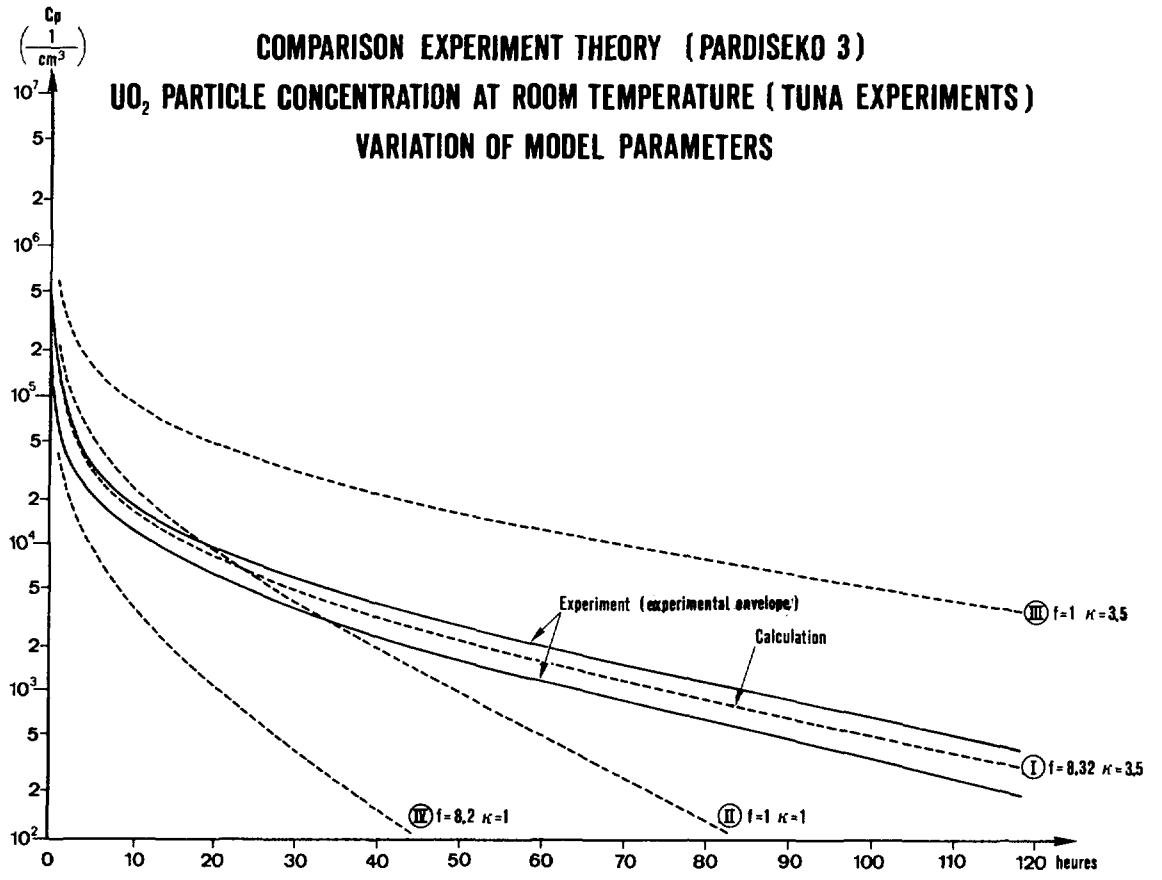
COMPARISON EXPERIMENT THEORY (PARDISEKO 3)
UO2 PARTICLE CONCENTRATION AT ROOM TEMPERATURE (TUNA EXPERIMENTS)
VARIATION OF MODEL PARAMETERS
Cp (1/cm3)
Experiment (experimental envelope)
Calculation
III f=1 κ=3,5
I f=8,32 κ=3,5
IV f=8,2 κ=1
II f=1 κ=1
heures

Fig. 13

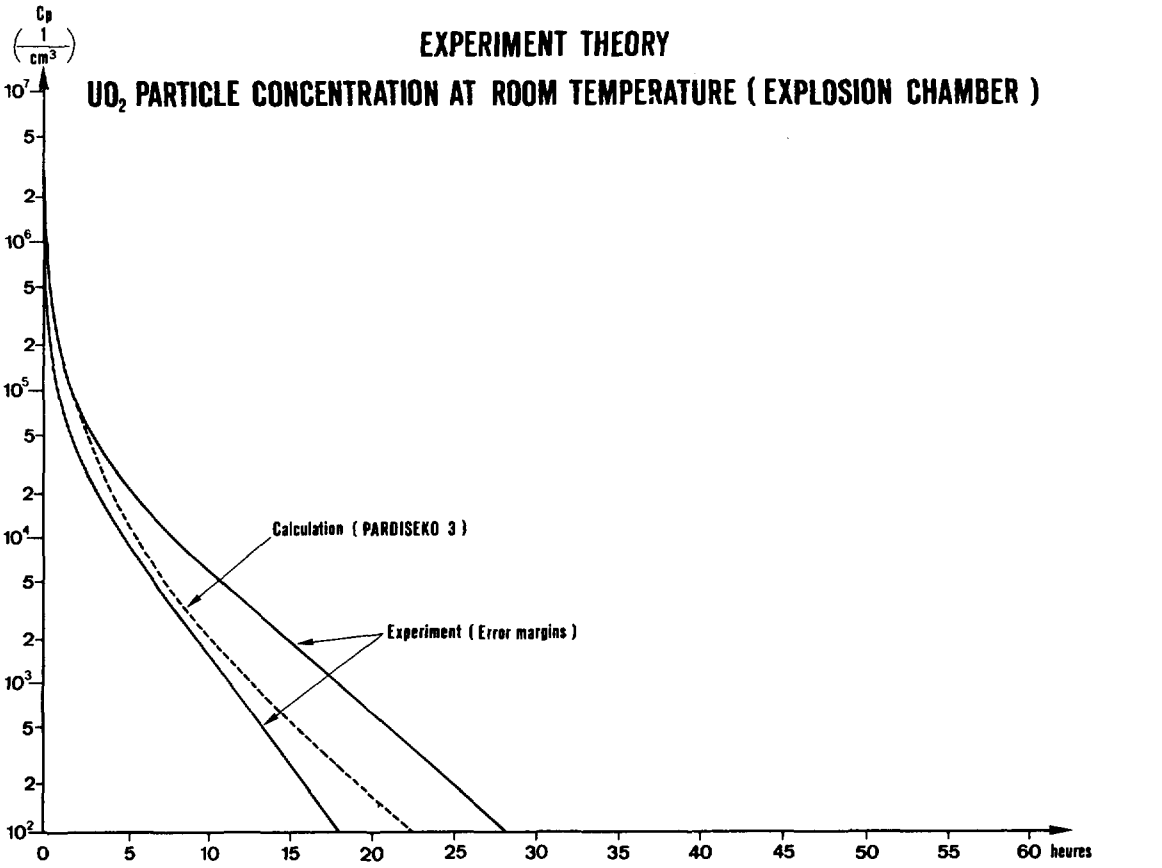
EXPERIMENT THEORY
UO2 PARTICLE CONCENTRATION AT ROOM TEMPERATURE (EXPLOSION CHAMBER)
Cp (1/cm3)
Calculation (PARDISEKO 3)
Experiment (Error margins)
heures

Fig. 14

Fig : 15

COMPARISON PARDISEKO 3 - HAARM 2
SIZE DISTRIBUTION OF THE SUSPENDED PARTICLES

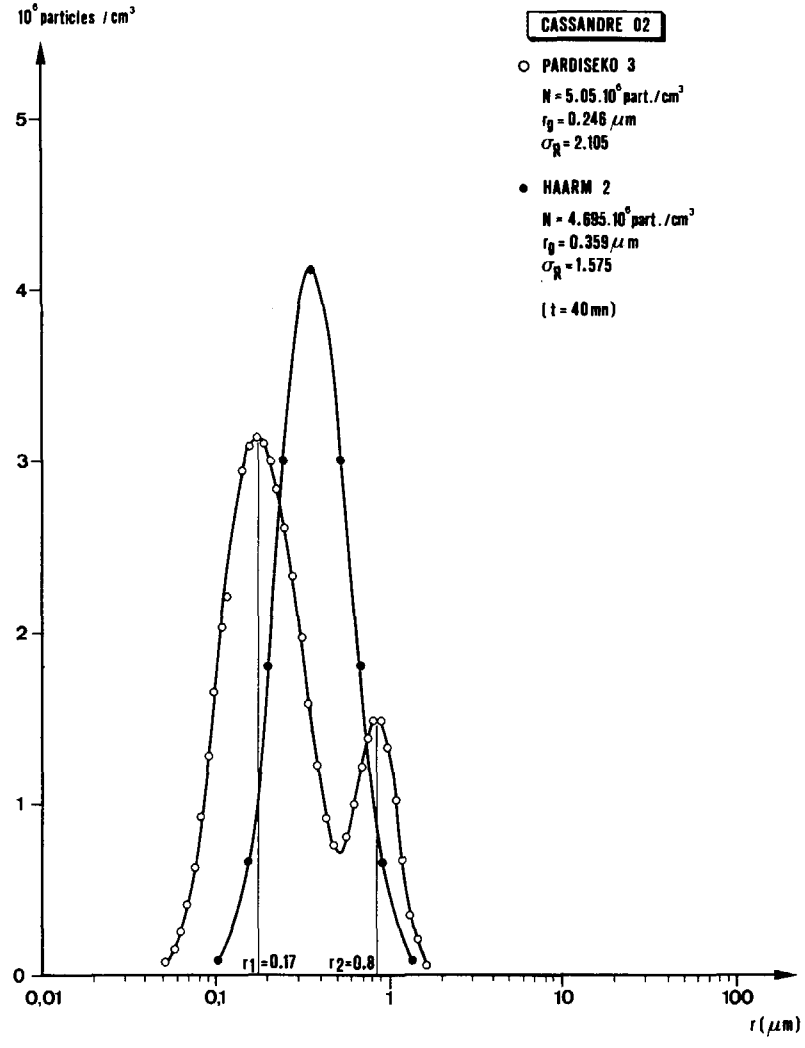

Fig : 16

COMPARISON PARDISEKO 3 - HAARM 2
SIZE DISTRIBUTION QF THE SUSPENCED PARTICLES

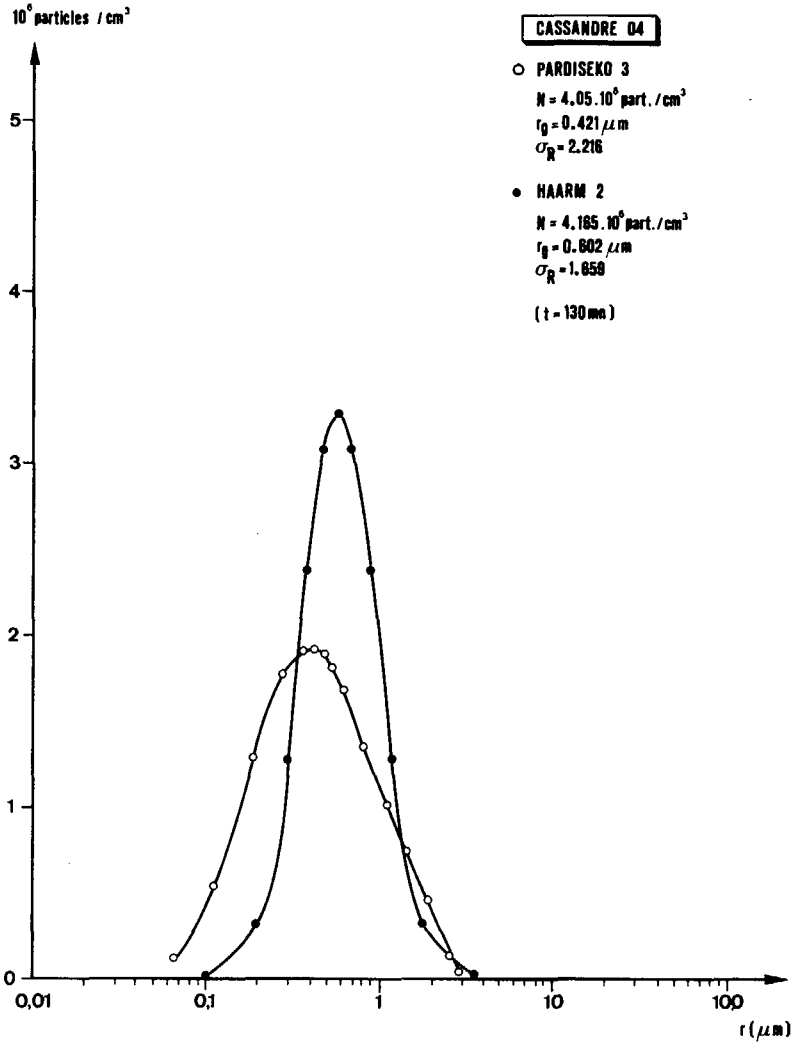

Fig. 17

CASSANDRA 4 COMPARISON
PARDISEKO 3, PARDISEKO 3b, HAARM-2

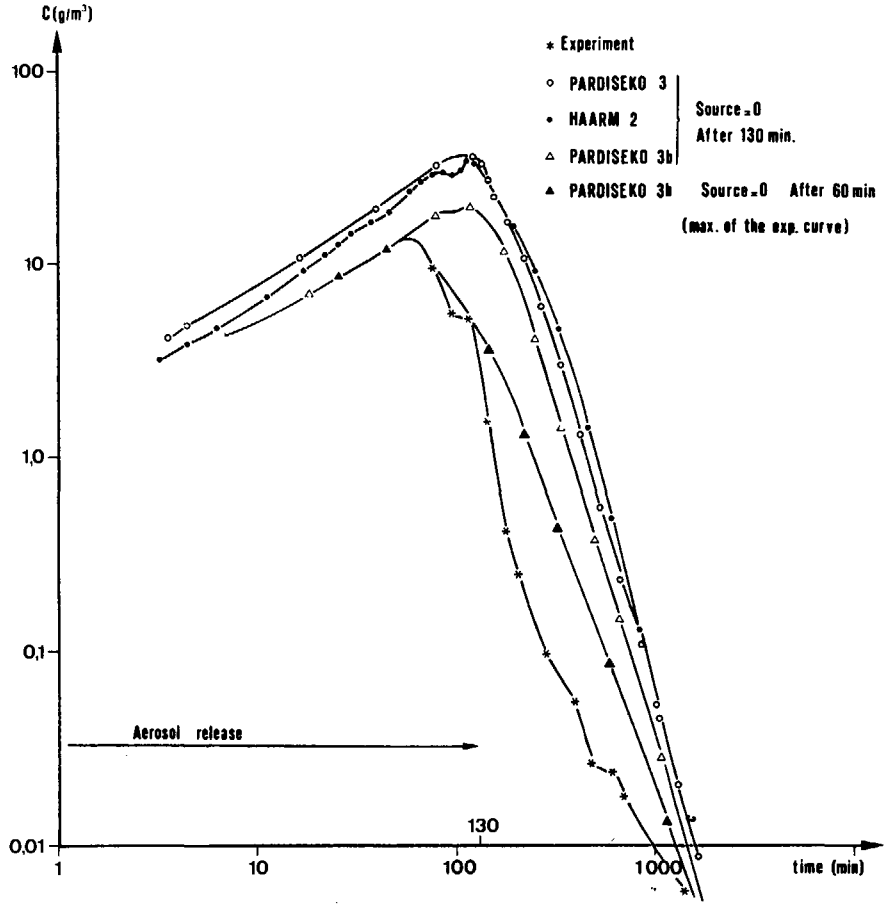

COMPARISONS OF HAA-3B PARDISEKO III AND AEROSIM CALCULATIONS

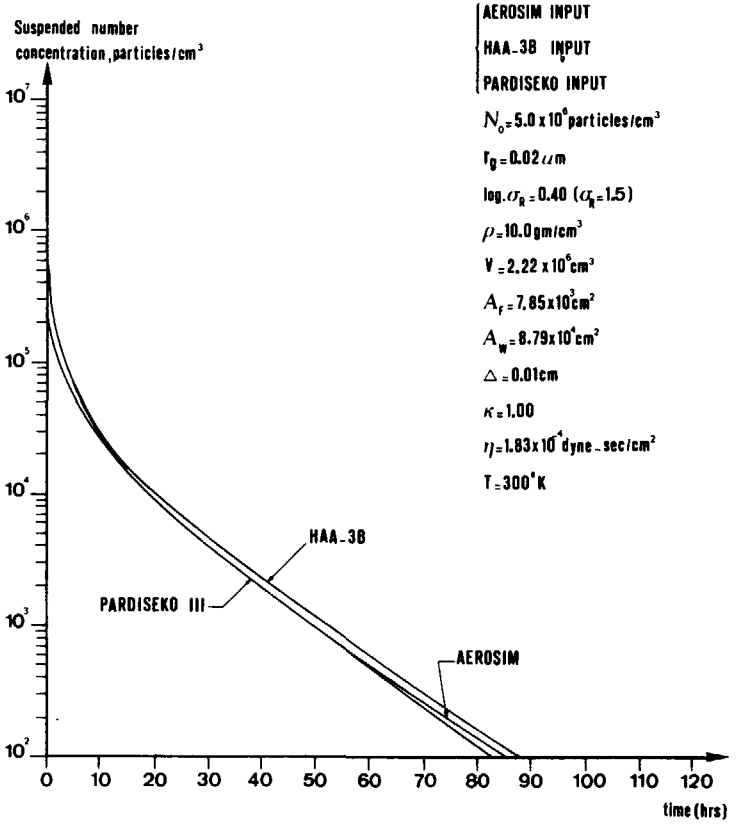

Fig.:19

TIME LAPSE CHANGE OF Na_2O AEROSOL CONCENTRATION FOR THE CALCULATED AND THE EXPERIMENTAL RESULTS IN THE CHAMBER

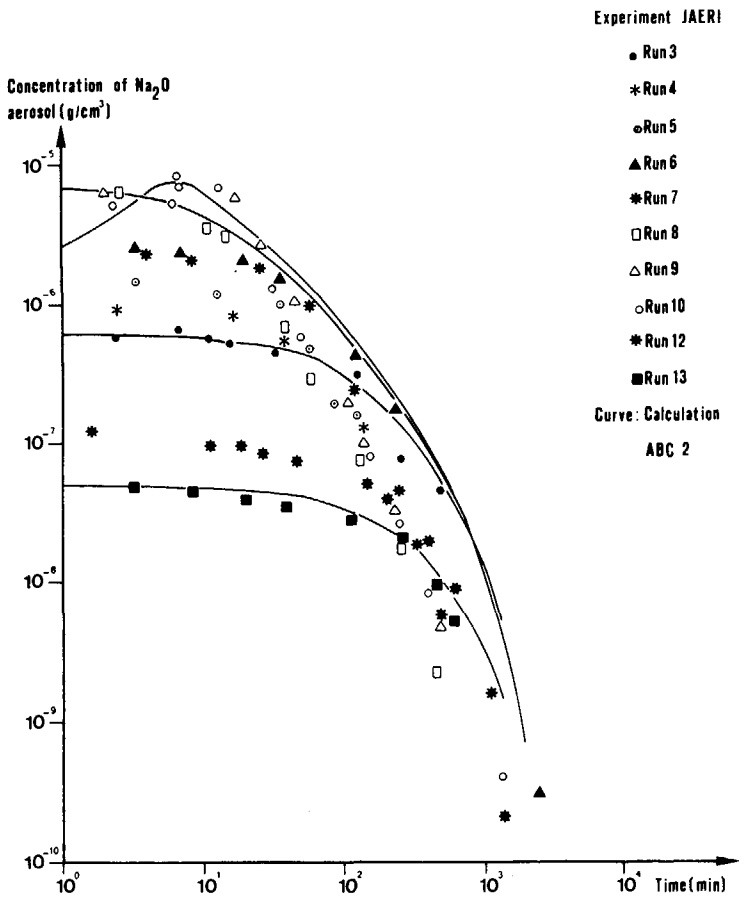

COMPARISON WITH AI LTV EXPERIMENTS AND CALCULATION FOR SODIUM OXIDE AEROSOL CONCENTRATION

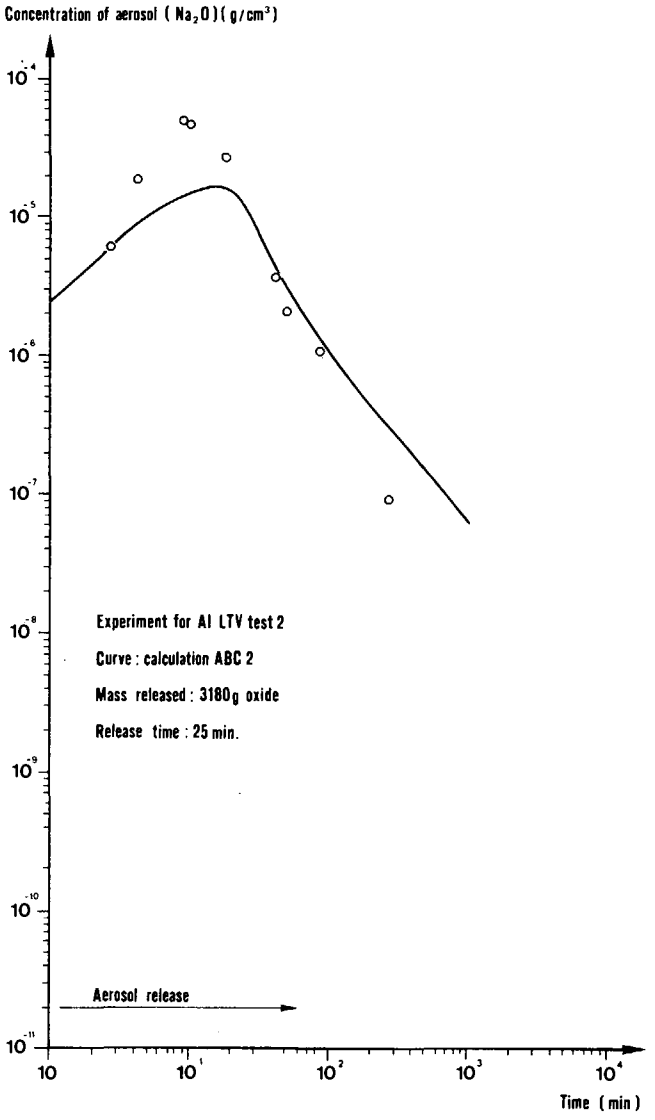

Fig : 21

COMPARISON OF AI LTV EXPERIMENTS AND CALCULATION FOR SODIUM OXIDE AEROSOL CONCENTRATION

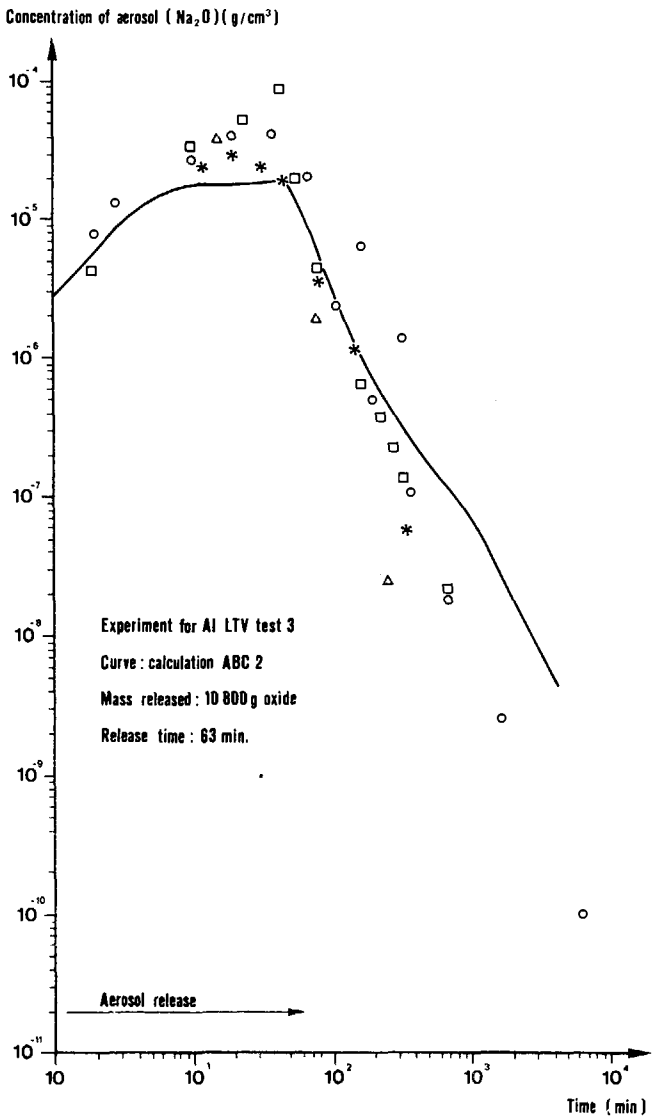

Fig.22

SETTLED AND PLATED MASS OF SODIUM OXIDE VS. TIME FOR AI LTV TEST 3 AND CALCULATION (ABC 2)

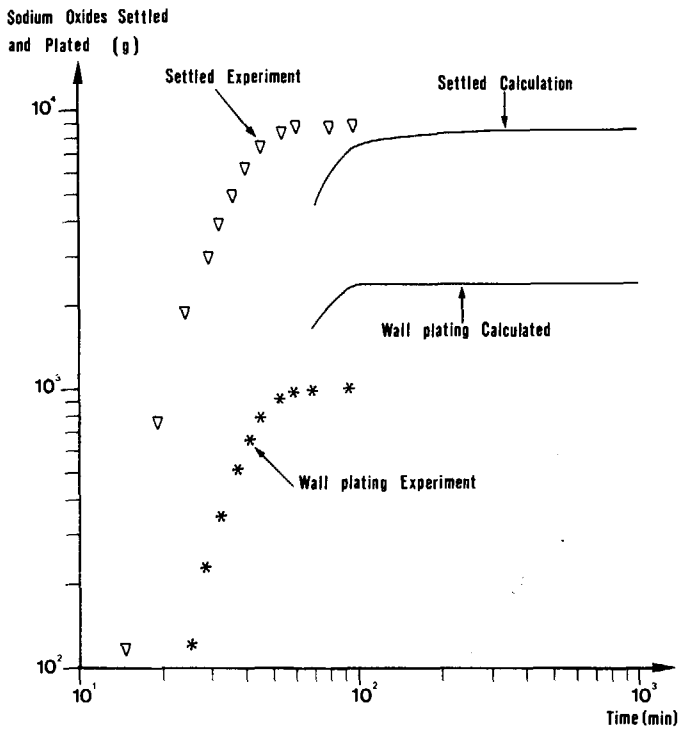

Fig. 23

CONCENTRATION DECREASE OF URANIUM OXIDE (U_3O_8) AEROSOL

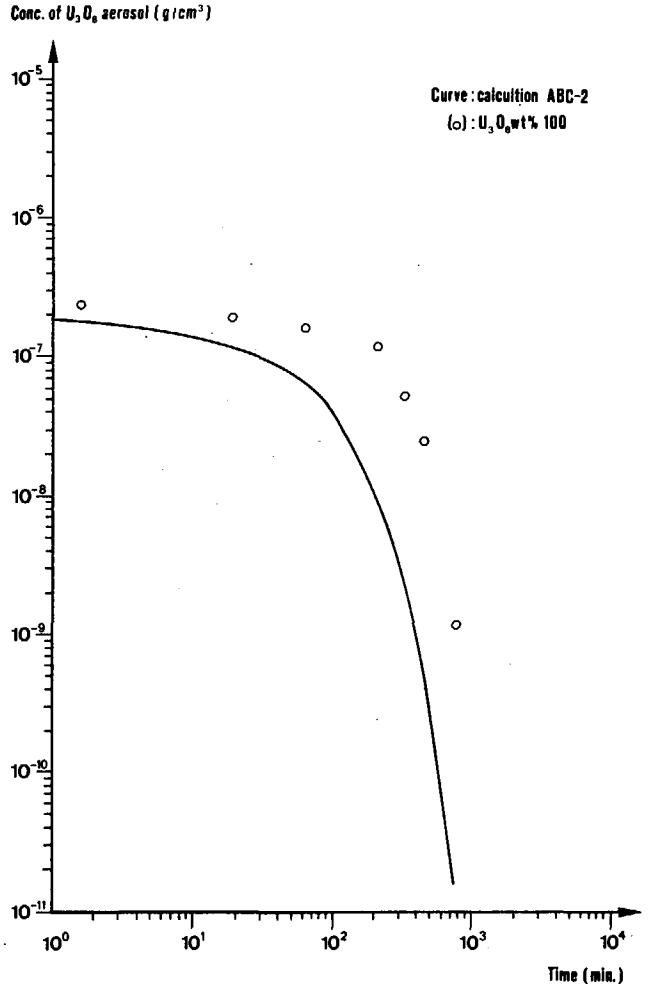

Fig. 24

CONCENTRATION DECREASE OF MIXED Na_2O-U_3O_8 AEROSOL IN THE CASE OF U_3O_8 CONTENT OF 6,7 Wt %

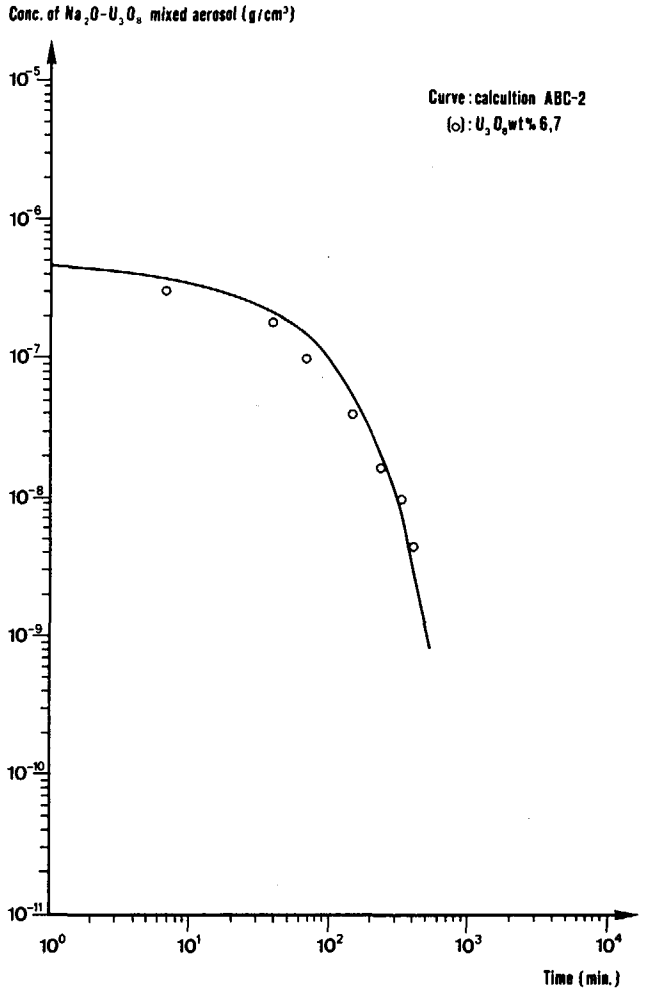

Fig. 25

CONCENTRATION DECREASE OF MIXED $Na_2O-U_3O_8$ AEROSOL IN THE CASE OF U_3O_8 CONTENT OF 85 Wt % IN THE CHAMBER

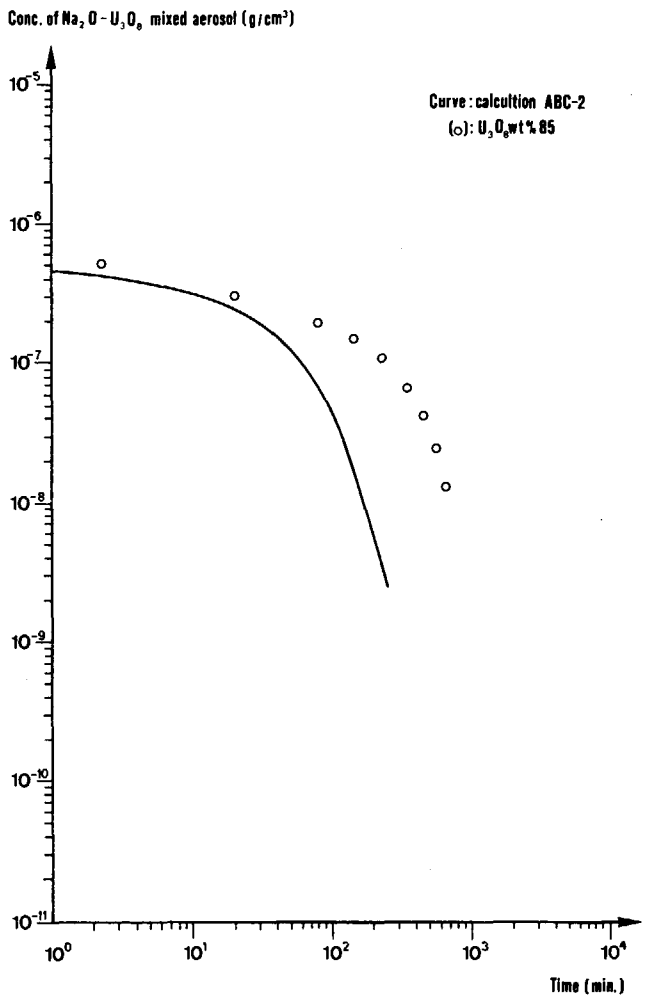

Fig:26

CHIMNEY TYPE CHAMBER

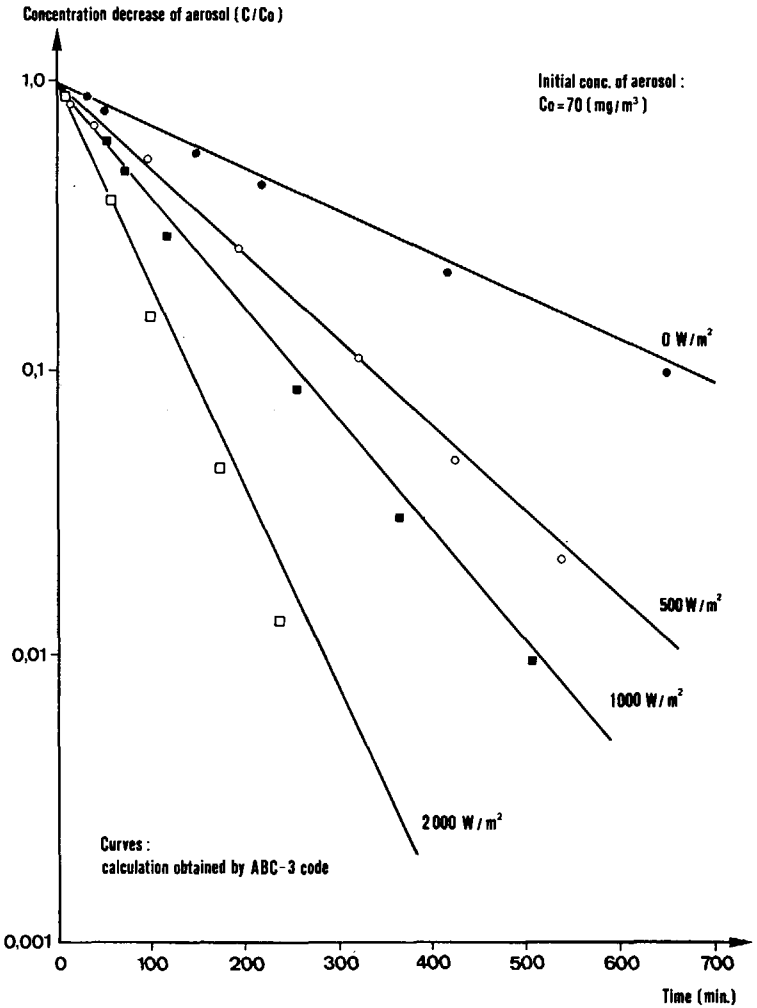

Fig:27

HOT-PLATE HEATING

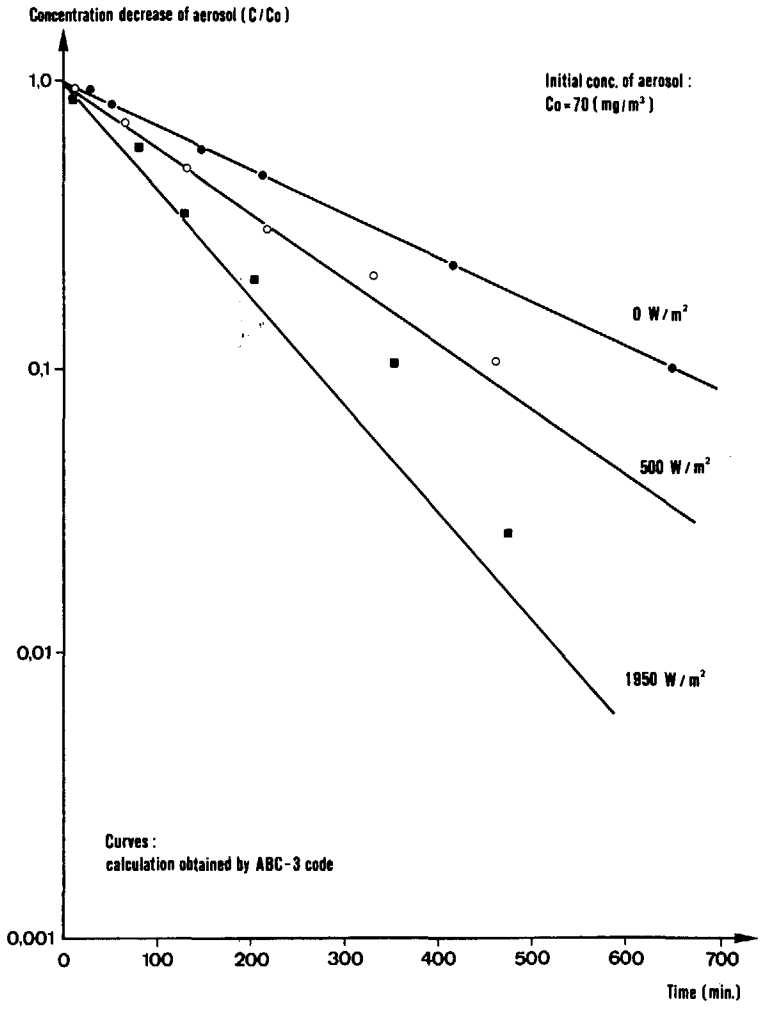

Fig. 28

CHIMNEY-TYPE CHAMBER

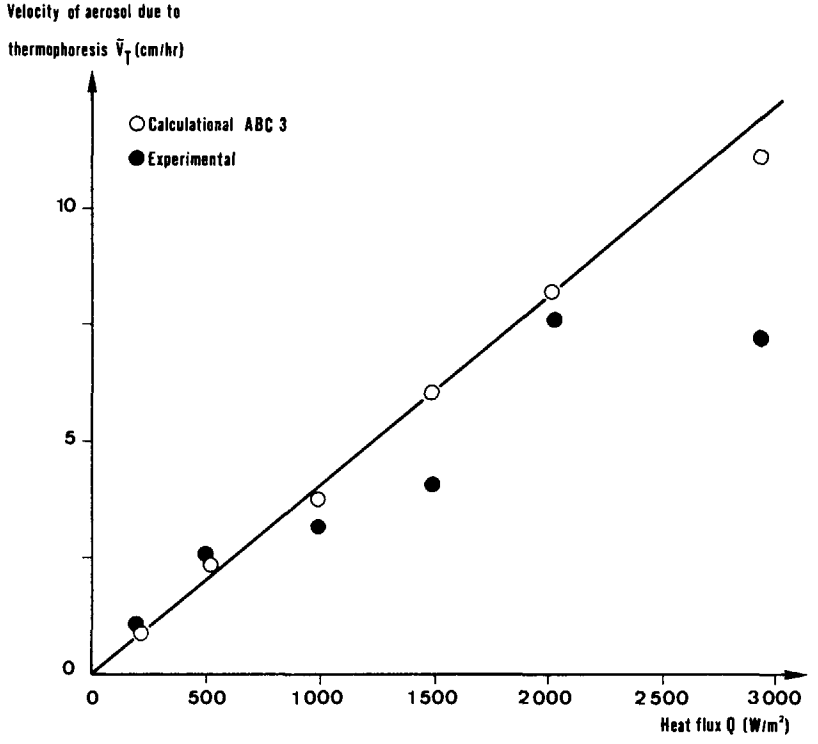

Fig: 29

DECAY CONSTANTS β (IN SEC^{-1}) OF GOLD AEROSOLS
FOR VARIOUS VESSELS AND HEATING GEOMETRIES
AS A FUNCTION
OF SPECIFIC HEATING POWER Q/V (IN $W.cm^{-3}$)

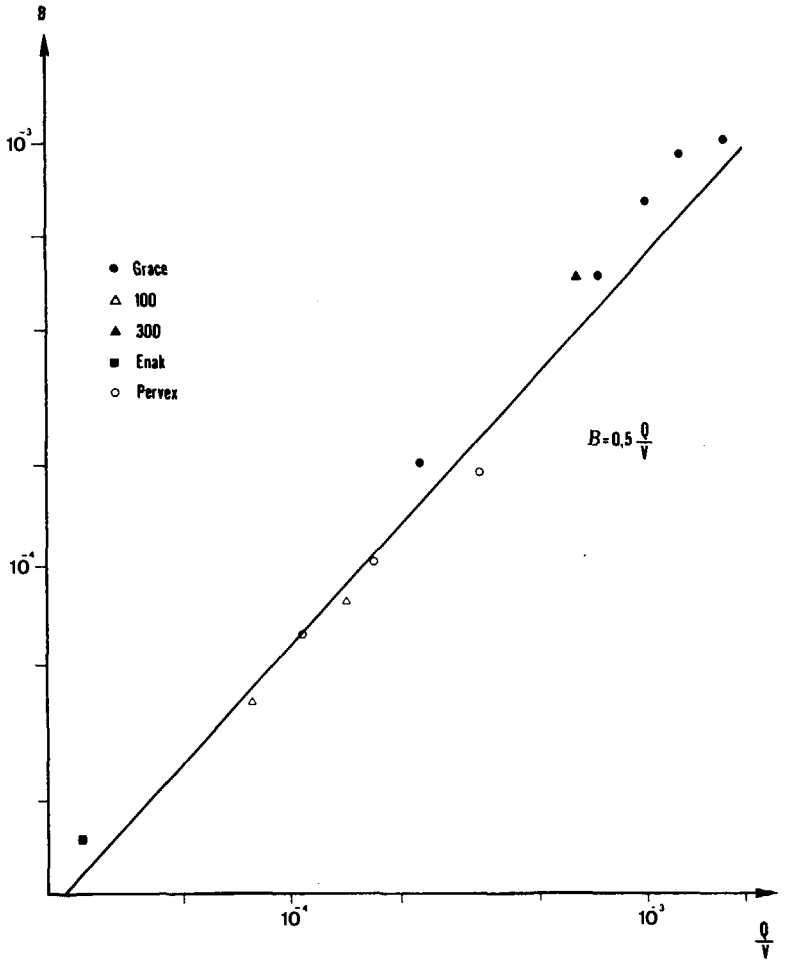

DECAY CONSTANTS β (IN SEC^{-1}) OF GOLD AEROSOL IN PERVEX
THE FLOOR WAS HEATED WITH A VARIABLE POWER Q (IN WATTS)

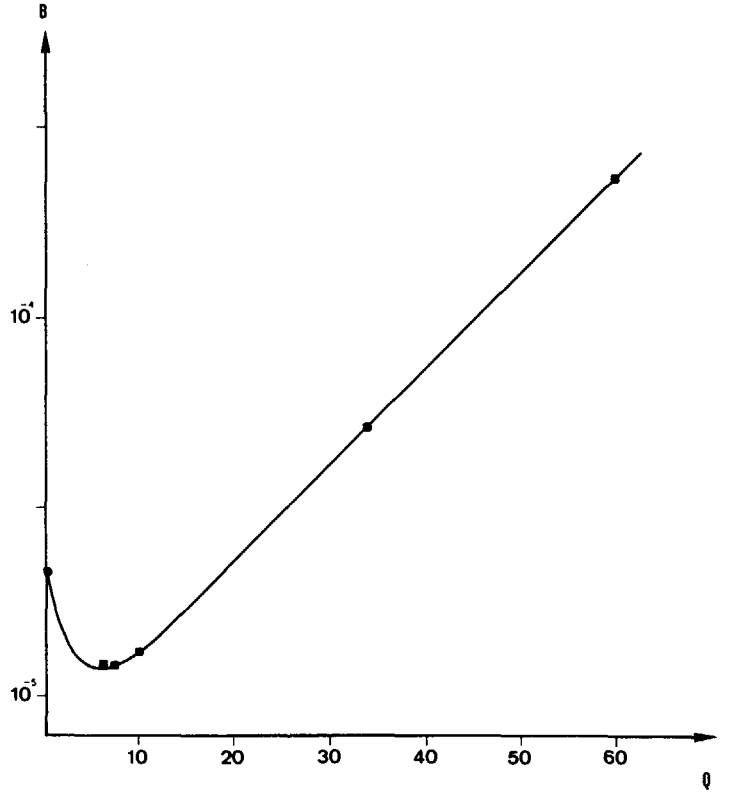

Fig. 31

MASS CONCENTRATION DECAY (c_m IN mg.m^{-3}) OF GOLD AEROSOL IN PERVEX WITH WATER LAYER ON THE FLOOR (•) AND UNDER DRY CONDITIONS (○) 60 W FLOOR HEATING POWER

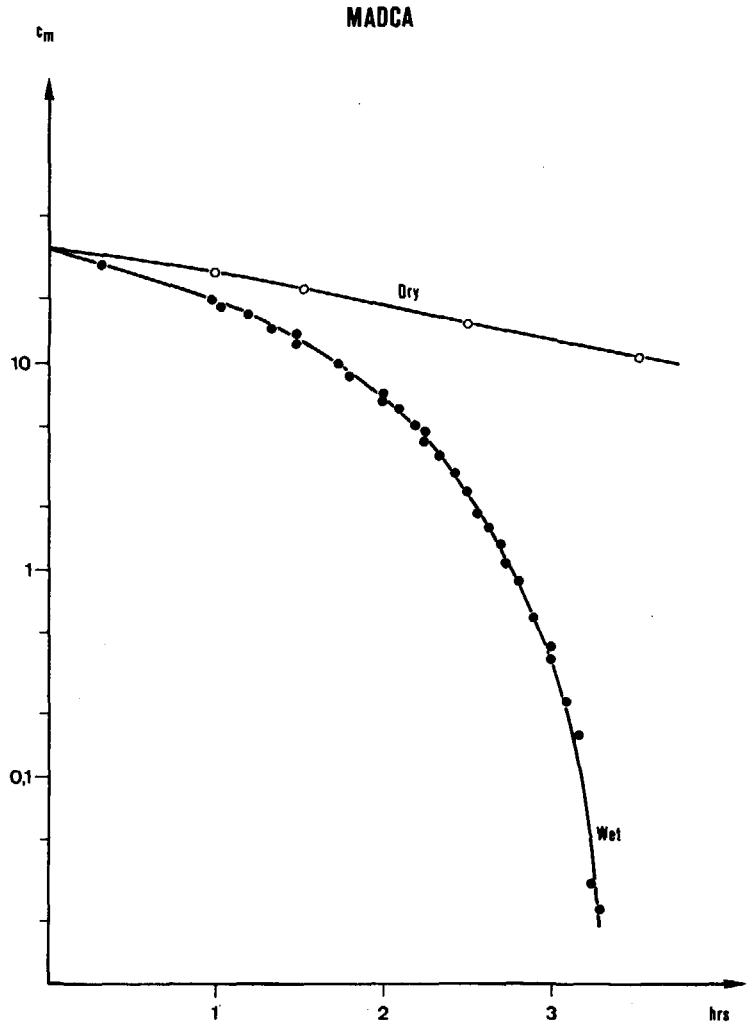

Fig: 32

DECAY OF AEROSOL MASS CONCENTRATION (c_m IN mg.m^{-3}; t IN MINUTES) IN GRACE AND PERVEX FOR VARIOUS HEATING POWER LEVELS OF WATER LAYER

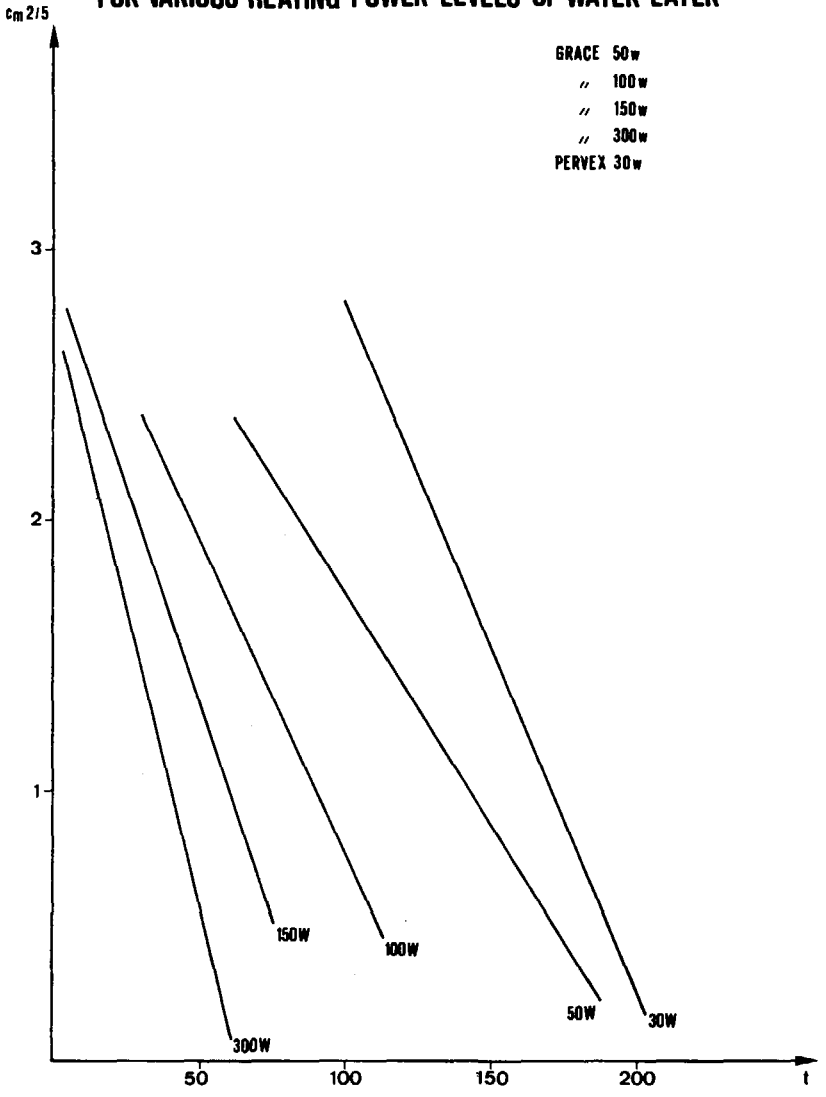

Fig:34

DECAY OF AEROSOL NUMBER CONCENTRATION
(c_n IN ARBITRARY UNIT) IN SAUNA
WITH HEATED SODIUM POOL AT TWO LEVELS
OF HEATING POWER

DECAY OF AEROSOL MASS CONCENTRATION (c_m IN mg.m^{-3}) IN SAUNA
WITH HEATED SODIUM POOL AT VARIOUS HEATING POWER

	5kW	1kW
Na	335'	523'
gas	252'	405'
walls	230'	357'

Fig:33